**Mohamed Khider University of Biskra**

**Faculty of Exact Sciences and Nature and Life**

**Department of Matter Sciences**

# Master Dissertation

Sciences of Matter

Physique

Physique of Materials

Réf. :

---

Presented by:

**DJEHAICHE NOUR EL HOUDA**

## *Effect of Niobium doping on the properties of Titanium Dioxide ($TiO_2$) Thin films elaborated by Sol-Gel (Spin-coating).*

---

**Jury :**

| | | | |
|---|---|---|---|
| Nouadji Malika | MCA | Université de Med Khider | President |
| Saidi Hanane | Pr | Université de Med Khider | Reporter |
| Attaf Abdallah | Pr | Université de Med Khider | Examiner |

Academic Year: 2018 – 2019

# Acknowledgements

Firstly, I want to thank Allah Almighty who gave me the strength and courage to carry out this modest work.

Then I express my deep gratitude to my parents for their encouragement, support and sacrifices.

After that, I make a point of profoundly thanking my supervisor Mrs Saidi Hanane, Professor at the University of Biskra, She has been a great support on all fronts and made my master dissertation journey a memorable experience. And I would like to extend my sincerity and gratitude to my teacher " Mister Attaf Abdallah" for his patience, his guidance, and his invaluable support, in order to carry out my Work well .

I sincerely thank all my teachers for their help during my study.

I thank also all the members of thin films‟ laboratory of our university in particular: Ch. Saadia, D. Mohamed, B. Youcef, M. Radhia, and also B.Okba who with them I have realized this work.

I would like to thank my friends and also to thank the jury numbers who have accepted to judge this work.

# Table of contents :

Chapter 3. Experimental procedures, Results and discussions.

# General introduction

The study of matters in the form of thin films has been the subject of a growing number of studies since the second half of the 20$^{th}$ century due to advances technological in the development and the characterization of these layers. TCO materials are increasingly used in new applications and occupy an increasingly important place in our lives. They are at the base of a new scientific and technological revolution **[1]**.

During the last years, Transparent Conducting Oxides (TCO) were the subject of numerous research works **[2]**. Among the TCO, Titanium Oxide $TiO_2$ has an interesting properties (high chemical stability, high refractive index and transparency in the visible .....) that allow to use it in several applications: photocatalysis, gas capture, and dye solar cells **[3]**.

To obtain the thin layers of $TiO_2$, deferent deposition techniques have been used among the techniques using the Sol-Gel technique. this process is effective in the production of homogeneous thin layers with high purity. In order to improve of $TiO_2$ properties thin films, we change some parameters such as doping concecentration.

This work focused on the elaboration and characterization of Niobium doped Ttitanium Oxide ($TiO_2$: Nb) thin films by Sol-Gel (spin coating). The aim of this work is to improve the Structural, Optical and Electrical properties of $TiO_2$ thin films as function Niobium doping concentration for photovoltaic applications.

The work described in this memory is presented in 3 chapters, as follows:

The first chapter will include bibliographic research on Titanium Oxide, its properties and its applications. then we talked about Niobium as a doping element.

In second chapter will deal, the thin film deposition techniques and tools of characterizations (Structural, Electrical and Optical) and different methods of the deposit characteristics calculation (the grains size, the thickness, the Optical gap, and Disorder...) will be discussed.

In the third chapter, will present the description of the various stages in the development of thin films of titanium oxide by the Sol-Gel method and summarizes obtained experimental results of this work concerning the effect of the doping concentration by Niobium and the corresponding discussions.

In the end, we finish our work with a general conclusion and some tracks to complete.

# Chapter 1:
# Generalities about Titanium Dioxide TiO2

In this chapter, firstly we present a bibliographic study on Transparent Conducting Oxides (TCO) and especially Titanium Dioxide ($TiO_2$) with their main properties. Then, we talk about of Titanium Dioxide applications. Finly we talk about of Niobium element as a doping element.

## I.1 : Definition of Transparent Conducting Oxide :

Transparent Conducting Oxides (TCOs) constitute a unique class of materials, which combine two physicals properties together, high optical transparency and high electrical conductivity. These properties are generally considered to be mutually exclusive of each other since high conductivity do metals possess a property while insulators are optically transparent. This peculiar combination of physical properties is achieved by generating free electron or hole carriers in a material having a sufficiently large energy band gap (i.e., > 3.1 eV) so that it is non-absorbing or transparent to visible light.

The charge carriers are usually generated by doping the insulator with suitable dopants and by defects. It is no wonder that this unique material property makes TCOs an important material in technology and useful in commercial applications **[4]**.

## I.2 : Definition of thin films :

Thin films are just thin layers of material and generally less than 1 μm thick. Thin film devices would generally be about 5 to 50 μm thick. If growth is one atom per atom or molecule per molecule, it is called a thin layer, and if growth is grain by grain, it is thick films **[5]**.

A thin film is a thin film of a material deposited on another material, called a "substrate". The purpose of the thin layer is to give particular properties to the surface of the part while benefiting from the massive properties of the substrate for example:

- Electrical conductivity: metallization of the surface, for example; to observe an insulating sample under a scanning electron microscope.
- Optics: tain mirror, anti-reflective treatment of camera lenses, nickel plating of fire helmets to reflect heat (infrared), gilding of their visor to avoid glare.
- Economical: development of electronic components with little technological step **[6]**.

## I.2.1 : Thin film growth mechanisms:

In a large number of deposition techniques, thin film growth is atom by atom (or molecule by molecule). The formation of the thin film is divided into four stages **[7]**:

1. The condensation.
2. Nucleation.
3. Coalescence.
4. The growth.

## I.2.2 : Nucleation and growth :

The process of the film formation starts while the substrate was exposed to a flux of material. Atom which came to the surface from chemical bonds with atoms of substrate. Also, the mobility of the sputtered atoms on the surface is relatively high, therefore they are settling down on the equilibrium positions **[8]**.

Several models have been suggested for the description of the film growth:

1) **Frank – van der Merve growth mode or layer by layer growth mechanism :**

The layer-by-layer growth mechanism of Frank-van der Merwe happens when film atoms bind more to the substrate than with each other. The growth of the next layer does not begin until the complete formation of the previous one is finished, so there is a distinctly two-dimensional growth.

2) **Vollmer – Weber growth mode or mechanism of island growth :**

Mechanism of island growth happens when atoms in the film bind more with each other than with the substrate surface. In this case three-dimensional islands are created and grow directly on the substrate surface.

3) **Stranski – Krastanov growth mode :**

This mode is a combination of the previous two. It describes the case when the growth starts as two-dimensional (layered) and then change to a three-dimensional (island). After completion of the two-dimensional layer growth the three-dimensional island growth occurs. The nature and thickness of the two-dimensional layer (often referred to as a Stranski – Krystanov layer) depends on the individual case **[9]**.

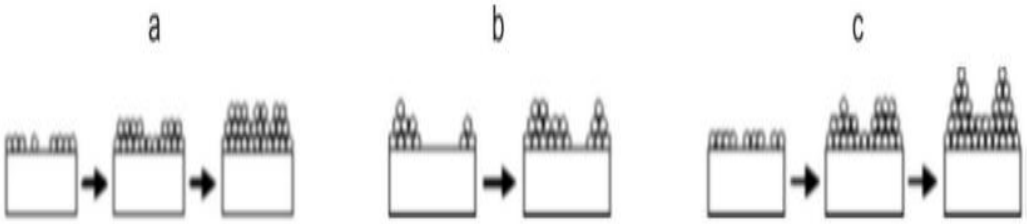


Figure I.1 : Representative Diagram of Three Growth Modes [9].

## I.3 : Generalites about Titanuim Dioxide :

### I.3.1 : Definition of Titanuime Dioxide :

Titanium Dioxide is a chemically stable, non-toxic, non-volatile material non-flammable and biocompatible, which can be found in many applications because it has several interesting properties. Due to its optical properties and non-toxicity $TiO_2$ is used for example as an anti-UV screen in sun creams **[10]**.

Its electrical properties are no less varied. When his composition is stoichiometric, $TiO_2$ behaves like an insulator, while some defects are enough to make it n-type semiconductor (oxygen vacancy, interstitial atom of titanium) **[1]**. It is obtained from titanium ore. Approximately 95% of the amount of ore mined is used for the production of the pigment and only 5% for the preparation of the metal **[11]**.

Titanium Dioxide has a particularly high refractive index and its insensitivity to visible light, because of its wide bandgap (3.2 eV) only allows it to absorb in the near ultraviolet. It presents for the spectrum of visible light a coefficient of very high diffusion without absorption zone **[12]**.

Table I.1 : The characteristcs of Titanium Dioxide in the macroscopie state.

| Chemical formula | Titanium Dioxide |
|---|---|
| **Appearance** | **Solid white (powder), very bright** |
| **Odour** | **Odorless** |
| **Brute formula** | **$TiO_2$** |
| **Molar mass** | **79.890 $g.mol^{-1}$** |
| **Volumetric mass** | **3.9 to 4.3 $g.cm^3$** |
| **Solubility** | **Insoluble in water / organic solvents** |
| **T° of Fusion** | **1855 °C** |
| **T° Boiling point** | **2755 °C** |

## I.3.2 : Choice of $TiO_2$ :

Titanium Dioxide is a cheap material, widely used in many applications such as waveguides, anti-glare layers in conversion photovoltaic and electrochromic systems because it has many properties interesting (excellent mechanical hardness, good chemical stability, high refraction, good transparency in the visible and near infrared domains...) **[13]**.

## I.3.3 : Titanium Dioxide properties :

### I.3.3.1 : Structural properties:

$TiO_2$ exists in different crystalline forms : Rutile, Anatase, Brookite, more rarely the bronze variety ($TiO_2$-B) and phases obtained under high pressure. Only Rutile and Anatase phases play a role in $TiO_2$ applications.

#### a) The Anatase phase :

The structure of the Anatase phase is more complex than that of the Rutile phase **[14]**. Anatase is an insulator with a band gap of approximately 3.23 eV **[15]**. This structure is generally formed at lower temperatures than those of rutile formation and still brookite. Anatase is converted into Rutile at a temperature of about 800 °C **[16]**.

Furthermore, in the case of thin layers, the transformation temperature is different because it is dependent on the synthesis method used and even on the conditions of the experiment and the products that can be introduced there. For example the Sol-Gel method, generally the transformation occurs from 700 °C up to 1000 °C **[15]**.

Anatase shares almost the same properties as Rutile such as hardness and density. Moreover, it can also be considered as an n-type semiconductor **[17]**.

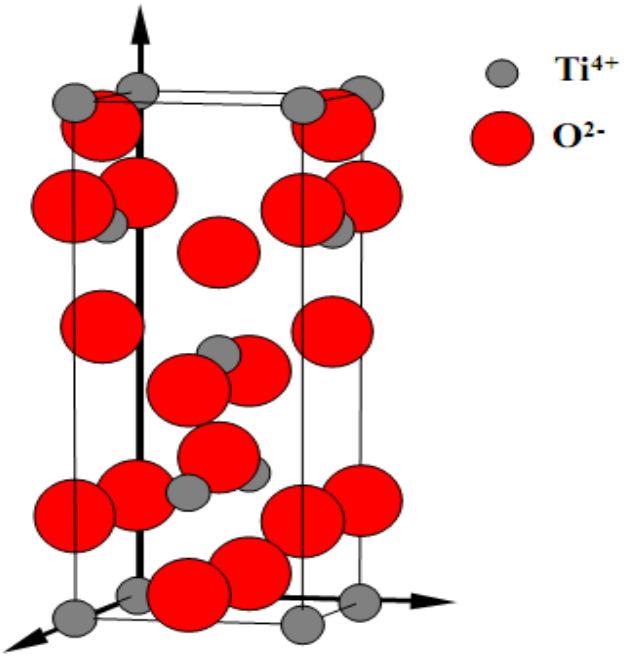


Figure I.2 : Structure of the Anatase phase of $TiO_2$ [18].

**b) The Rutile phase :**

Rutile is named after the Latin rutilus. The elemental cell of the phase is tetragonal symmetry in which each Titanium atom is in the center of a slightly distorted octahedron of oxygen atoms with four short Ti-O equatorial bonds (1.945 Å) and two longer apical bonds (1.979 Å). The sequence of these octahedrons is done either by edges or by vertices. The oxygen atoms are all bound to three Titanium atoms (two short bonds and one long bond) **[19]**. Although Rutile is an insulator, its electrical conductivity can be induced by the addition of small amounts of $Ti^{+3}$ **[20]**. Rutile has the most stable crystallographic form **[21]** of Titanium Dioxide and is produced at high temperatures **[20]**.

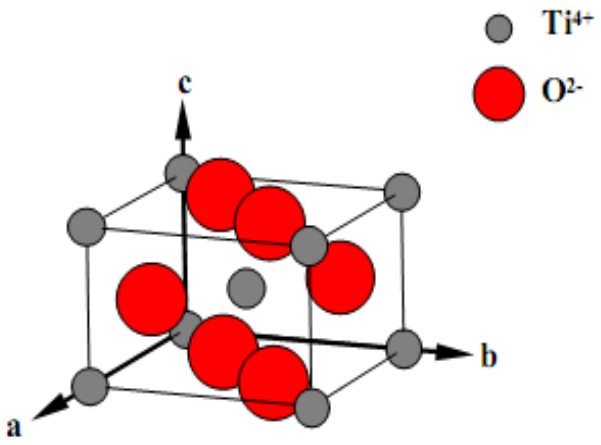


Figure I.3 : Structure of the Rutile phase of $TiO_2$ [18].

**c) The Brookite phase :**

The third metastable crystalline form of $TiO_2$ is Brookite of orthorhombic structure (Figure I.4) , its cell parameters are : a = 0, 546 nm ; b = 0.918 nm ; c = 0.514 nm.

The synthesis of pure Brookite is very difficult to achieve. Most studies on the synthesis of $TiO_2$ Brookite show the simultaneous presence of the Brookite, Rutile and / or Anatase phases. At high temperatures from 750 °C the Brookite is transformed Rutile. It has a density dm = 4.12 g / $cm^3$, intermediate between that of Anatase (dm = 3.89 g / $cm^3$) and Rutile (dm = 4.25 g / $cm^3$) **[22]**.

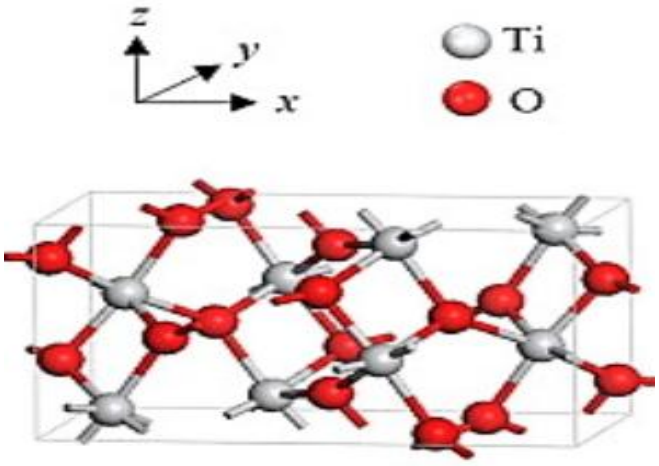


Figure I.4 : Structure of the Brookite phase of $TiO_2$ [23].

### I.3.3.2 : Optical properties :

The main use of Titanium Dioxide is due to its reflective properties of more than 96% of visible light .To achieve adequate reflectivity, $TiO_2$ particles must have a fine shape, size, and particle size distribution for maximum light reflection: the average particle diameter must be between 0.15 and 0.30 μm **[24]**. The hardness of the Titanium Dioxide does not make it possible to obtain the appropriate particle size distributions by simple crushing of large crystals, also this is the nucleation and the growth of these particles themselves, in elaborating processes, that are necessary control. Table (I.2) shows the values of the refractive index of the three crystalline phases of $TiO_2$ : Anatase, Rutile and Brookite **[15]**.

Table I.2 : Refractive indices of $TiO_2$ polymorphs.

| | Rutile | Anatase | Brookite |
|---|---|---|---|
| **Refractive index** | **2.61 - 2.89** | **2.48 - 2.56** | **2.58 - 2.70** |

### I .3.3.3 : Electrical properties :

Titanium Dioxide is an n-type semiconductor, the $TiO_2$ single crystals has a resistivity of about $10^{13}$ Ω.cm at room temperature, and about $10^7$ Ω.cm at 250 °C. These values are similar to reported conductivities for a Rutile single crystal: at 30 °C the conductivity was $5 \times 10^{-14}\ \Omega^{-1}\ .cm^{-1}$ while at 260 °C it was decreased to $3.3\times 10^{-9}\ \Omega^{-1}\ .cm^{-1}$.

Therefore, $TiO_2$ is generally considered an insulator at temperatures below 200 °C. There is a large number of applications for highly insulating $TiO_2$ films, including its use as a dielectric "gate" in devices MOSFET. However, the electrical properties of the $TiO_2$ film can be modified to become highly conductive for many applications such as: humidity and gas sensors **[25]**.

## I.3.4 : Equilibrium diagram of Ti-O :

The phase diagram of the TiO system described by Murray and Wriedt in 1987 (Figure I.5) shows a large number of different oxides between pure Titanium and Titanium Dioxide $TiO_2$, which is the stable, oxygen-rich stable phase. The Rutile may exist below 1800 °C temperature at which the Titanium Dioxide becomes liquid. While for temperatures to which the Titanium Dioxide becomes liquid. While for temperatures above 700 °C the Anatase changes allotropic form and becomes Rutile. The transformation temperature can be modified by adding impurities in the $TiO_2$. For example, the Anatase phase completely disappears at temperatures of about 530 °C, 680 °C and 830 °C for powder samples containing Vanadium, Molybdenum and Tungsten respectively **[26]**.

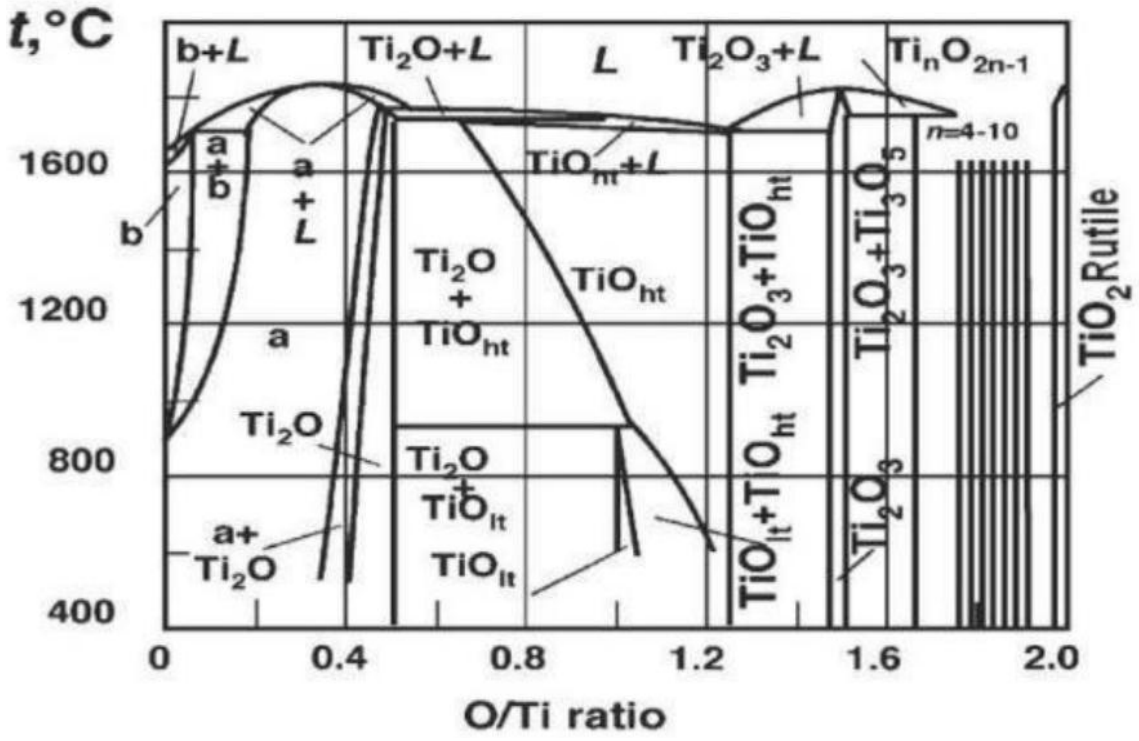


Figure I.5: Titanium-Oxygen balance diagram [20].

## I.4 : Applications of Titanium Dioxide ($TiO_2$):

There are many uses of Titanium Dioxide and especially in the following industrial sectors: cosmetics, abrasives, pulps, paints, stationery, surface treatments and electricity.

The scientific, industrial and high-tech applications of Titanium Dioxide are numerous, so thin films of $TiO_2$ are widely used in various applications. For example, we can cite: optical coatings, photovoltaic cells, gas sensors, electrochromic systems, self-cleaning of surfaces and catalysis. Titanium Dioxide is also used as a white pigment or as an anticorrosive protective coating for ceramics and electrochromic devices **[27]**.

Titanium Dioxide is able to decompose organic molecules, which allows it to be used for the purification of water, air or surface cleaning **[28,29]**.

In the field of photochemistry, Titanium Dioxide allows the initiation of reactions such as photolysis of water **[30]**, photoreduction of Nitrogen **[31]** and purification of liquid and gaseous effluents **[32-34]**. Titanium Dioxide coatings have favorable properties for optical guidance, in particular for amplifying signals in films doped with rare earth ions or for modifying the refractive index of the glasses surface.

Being easily supported by the human body, it covers some bone prostheses, allowing the fibrous tissues to attach easily to its granular structure. Its electrical properties are no less varied. When its composition is stoichiometric, the $TiO_2$ has as an insulator, while some defects are enough to make it semiconductor **[27]**.

## I.5: Doping of Titanium Dioxide:

### I.5.1 : Niobium :

Niobium, also called "Columbium", of atomic number Z = 41 and atomic mass 93 is part of the transition metals. Its main oxidation state is (+ 4), but it can exist in the state (+2), (+ 3) and (+ 5). The chemical properties of niobium are similar to those of tantalum Metal, which in its pure state has many properties (ductile, superconducting) is used as an adjunct to various steels, especially for the manufacture of materials for chemical and electronic equipment, as well as in nuclear technology (fuel cladding).

Niobium is poorly reactive at room temperature; it does not oxidize in air until 200 °C, it is not attacked by acids except hydrofluoric acid, alone or in mixture with nitric acid.

It can be attacked slowly by the bases. Niobium reacts hot with the halogens fluorine, chlorine, bromine and iodine **[35]**.

### I.5.2: Anionic Doping:

Researchers in heterogeneous photocatalysis (the catalyst is a semiconductor) consider that Anionic doping is a prelude to a new generation of photocatalytic nanomaterials active under visible radiation. Photocatalytic activity in the visible has been noted in several studies on the Anionic doping of $TiO_2$: Nitrogen N-$TiO_2$, Carbon C-$TiO_2$ and Sulfur S-$TiO_2$ **[13]**.

### I.5.3 : Cationic Doping :

The doping of $TiO_2$ oxide with transition metals is one of the most important approaches and several doping works have been carried out with different metals: Iron, Zirconium, Cerium, Manganese, Chromium, Cobalt, Tungsten and Silver. The authors report that this type of doping cationic decreases the energy threshold of $TiO_2$ by reducing the width of its bandgap **[20]**.

# Chapter2:

# Thin films deposition techniques and characterization tools

In this chapter, we talk about deferent techniques of deposition and especially the technique of Sol-Gel (spin and dip-coating). Then, we talk about the used technique for characterizing of our samples. Finally, the deferent relation which used to analysis the structural, optical and electrical properties of elaborated samples are illustrated in this chapter.

## II.1 : Technique of depositing thin films:

The thin films of Titanium Dioxide are made by using a wide variety of synthetic techniques, due to various applications of this material. Depending on the nature of the process, the techniques that are used can be divided into two categories: chemical deposition and physical deposition. The classification of the most common thin film deposition methods can be represented as shown in Figure (II.1) **[36]**.

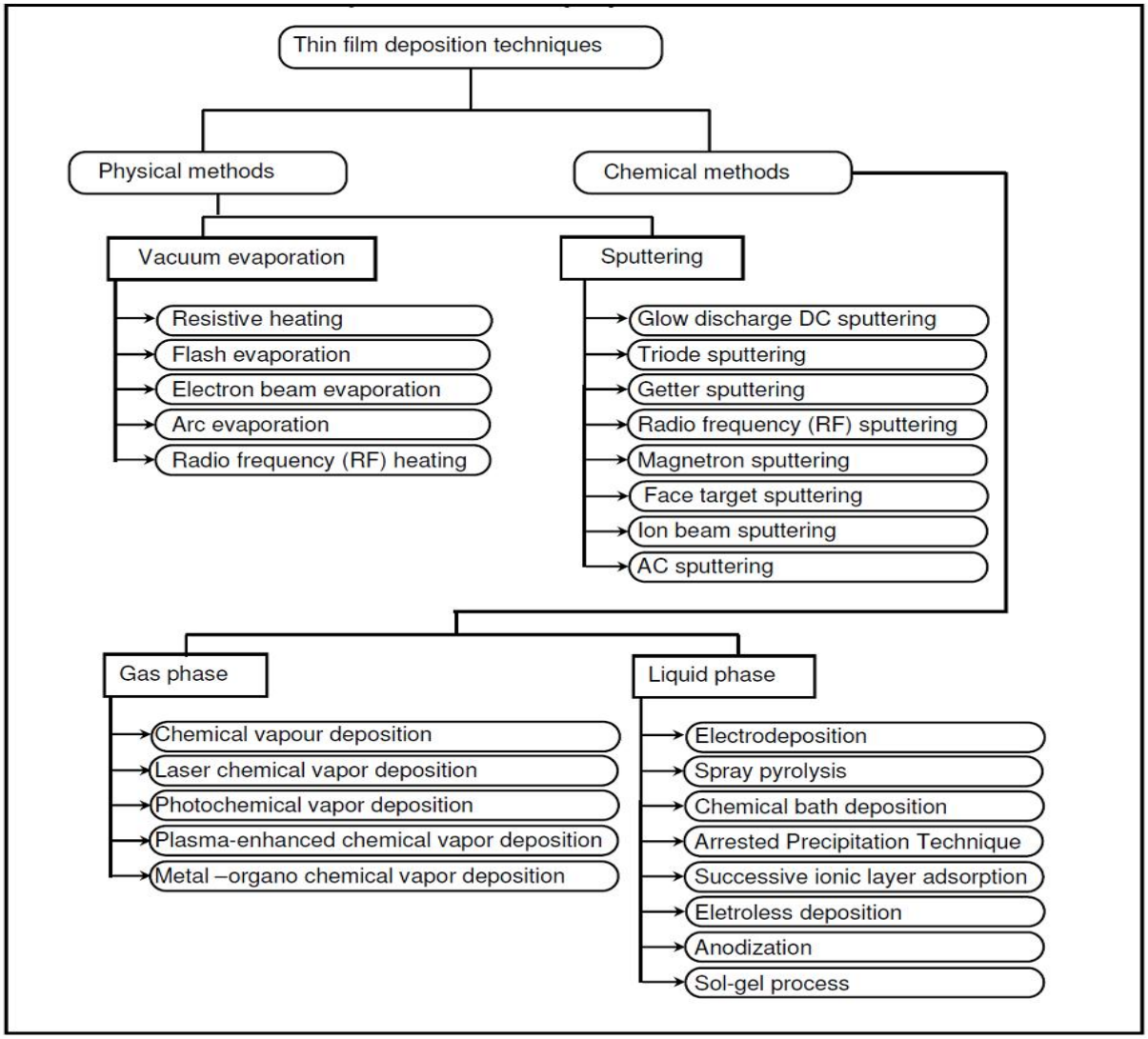


Figure II.1 : Classification of thin film deposition techniques [37].

## II.2 : Sol-Gel method:

### II.2.1 : Definition of Sol-Gel method:

The term Sol-Gel corresponds to the abbreviation "Solution-Gelation". Briefly, a "Sol" is a colloidal suspension of Oligomers whose diameter is only a few nanometers. Subsequently, this "sol" can be evolved through chemical reactions in a lattice with infinite viscosity, called "Gel" **[38]**.

The Sol-Gel process is based on the conversion of a liquid (the sol) into a solid phase (the Gel) by a series of chemical reactions of the hydrolysis and condensation type of the molecular precursors. solution of extreme purity. Many research groups use this process to produce materials with particular properties in various fields such as: chemistry, mechanics, electronics or optics, in different forms: powder, layer, solid, fiber (Fig.II.2) **[39]**.

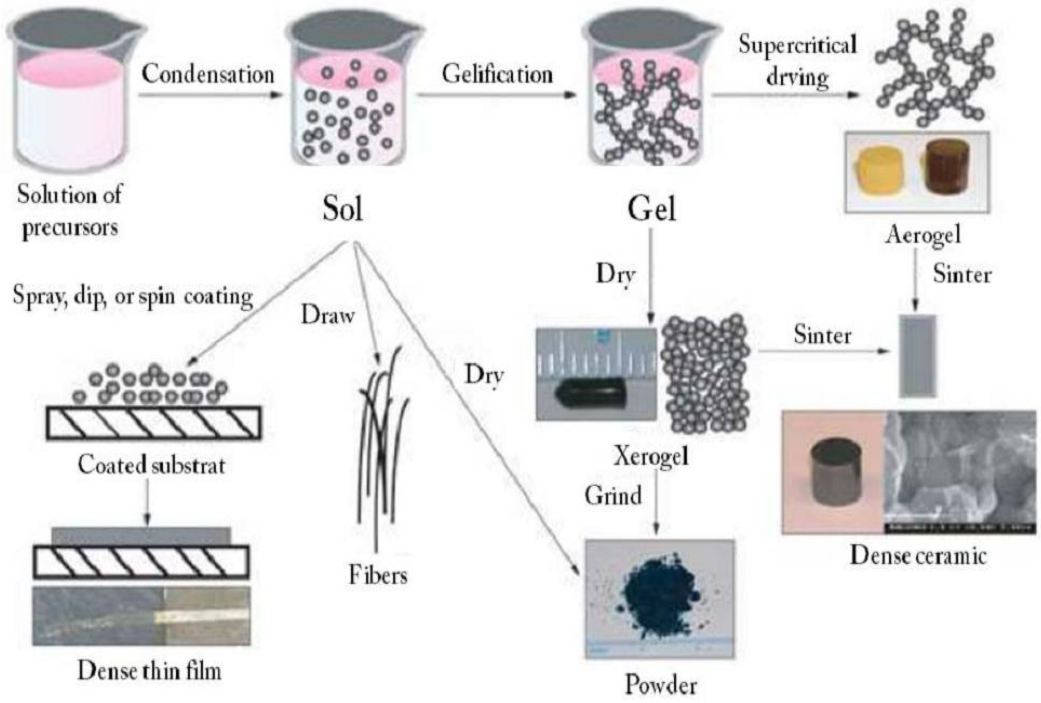


Figure II.2 : Schematic representation of the Sol-Gel process principle and the various possibilities of implementation [39].

The Sol-Gel method allows the elaboration of a large variety of Oxides in different configurations (monoliths, thin films, fibers, powders). This great diversity, both in terms of materials and formatting, made this process very attractive in areas of technology Such as Optics, Electronics, Biomaterials, Sensors (detection), separation media (Chromatography). Moreover, It has the advantage of using a soft chemistry and being able to lead to very pure or doped materials according to the intended application **[38]**.

### II.2.2 : The different Sol-Gel processes:

Several methods have been developed for shaping layers on a given substrate. Having each own characteristics, the choice of the deposition method depends on the characteristics of the substrate such as its geometry, its size but also its wettability (ability to receive a deposit) and its surface tension.

The Sol-Gel route essentially comprises two deposition processes: the centrifugation or spin-coating process and the dip-coating process **[40]**.

#### II.2.2.1 : Spin-Coating process:

This technique involves depositing a small amount of the solution in the center of a substrate. It will then be distributed over the entire support by rotating the latter until a uniform film is obtained (Fig II.3). This deposit method can be carried out in four phases:

1. The deposit of the solution.
2. The acceleration phase causes the flow of liquid towards the outside of the support.
3. Constant speed rotation allows ejection of the excess liquid in the form of droplets and the thickness reduction of the film uniformly.
4. The evaporation of the solvent which accentuates the decrease in the thickness of the deposited film.

The thickness of the film is inversely proportional to the speed of rotation but also depends on the viscosity of the solution and the rotation time **[36]**.

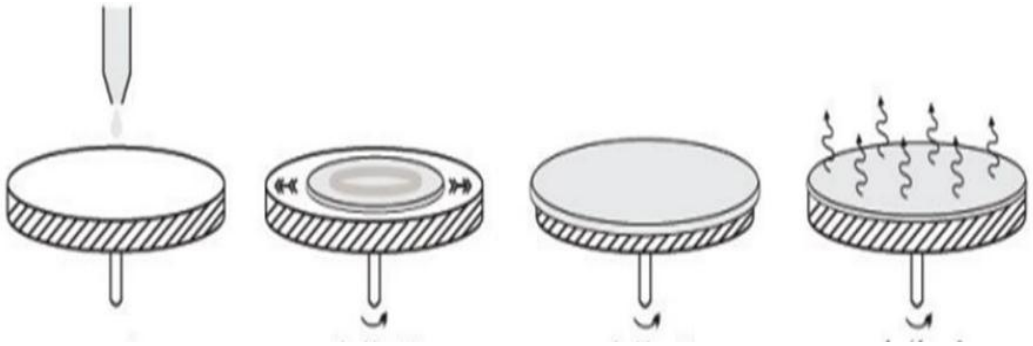

**Figure II.3 : The four steps of spin-coating [41].**

### II.2.2.2 : Dip-coating process:

One of most interesting aspects of the Sol-Gel technique is related to the possibility to employ the homogeneous solution obtained before the gelation in order to prepare thin films by means of the deposition techniques of spin and dip-coating. In this research project the dip-coating technique is used. The dip-coating technique can be described as a film deposition process where the substrate to coated is immersed in a liquid and then withdrawn with a well-defined speed under controlled temperature and atmospheric conditions. The coating thickness is mainly defined by the withdrawal speed, the solid content and the viscosity of the liquid. If the withdrawal speed is chosen, the sheer rates keep the system in the Newtonian regime, the coating thickness can be calculated by the Landau-Levich equation **[42]**.

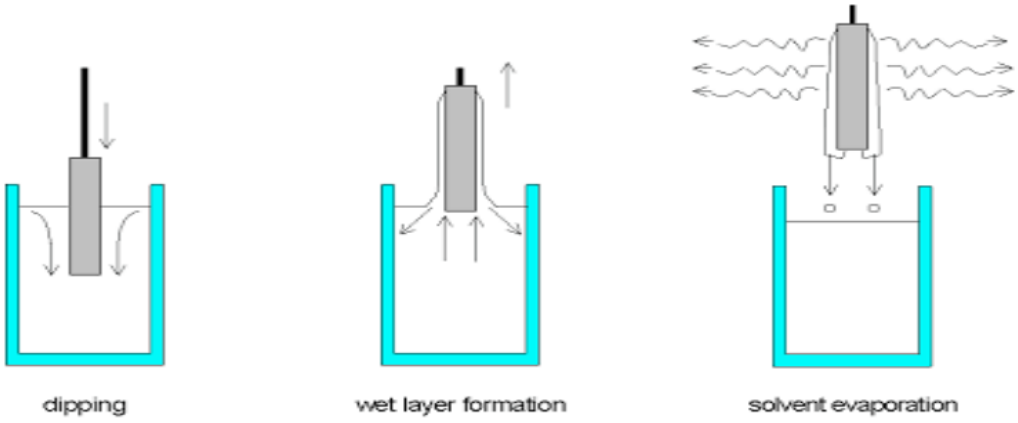


Figure II. 4 : The different stages of the dip-coating technique [4].

### II.2.3 : The precursors:

#### II.2.3.1 : Solution based on an organic precursor:

The most used organic precursors are metal Alkoxides of generic formula $M(OR)_Z$ or M denotes a metal of valence z and R represents a radical of an alkyl chain - ($C_nH_{2n+1}$).

The metal Alkoxides must be of high purity and have high solubility in a wide variety of solvents. This condition of high solubility can generally be achieved only in organic solvents **[43]**.

The main advantage of the use of organic precursors is to allow homogeneous and intimate molecular mixing of different precursors to produce multicomponent glasses and ceramics **[44]**.

#### II.2.3.2 : Solution based on an inorganic precursor:

The aqueous solution of mineral salt is used. In this solution, the $M^{Z+}$ cations are captured by molecules $H_2O$ polar molecules. A $(M\text{-}OH)^{(Z-1)+}$ bond is formed when an electron of a saturated orbital σ is transferred to a lower energy and unsaturated orbital. This is based on the following two partial reactions:

$$M^{Z+} + (OH)^- \leftrightarrow (M\text{–}OH)^{(Z-1)+} \qquad \text{(II.1)}$$

$$(M\text{–}OH)^{(Z-1)+} \leftrightarrow (M = O)^{(Z-2)+} + H^+ \qquad \text{(II.2)}$$

We know that according to the above-mentioned reactions in acidic medium by increasing the pH of the solution, one of the following two types of ligands can be formed:

- Hydroxo Ligand : $(M\text{–}OH)^{(Z-1)+}$
- Oxo Ligand : $(M = O)^{(Z-2)+}$

Condensation reactions involving hydroxo ligands : $(M\text{–}OH)^{(Z-1)+}$ lead to the formation of bonds (M-OH-M) or (M-O-M). Note, however, that stable colloidal solutions and gels can be achieved by keeping the pH constant. This route is mainly used in industrial processes for the manufacture of powders **[44]**.

### II.2.4 : Chemical reactions in the Sol-Gel process:

The reactions involved in the Sol-Gel polymerization process are essentially of two types: hydrolysis and condensation. They are triggered when the precursors are in the presence of water and they take place simultaneously **[36]**.

- Hydrolysis:

The hydrolysis corresponds to the initiation step of the hydro-condensation reaction process of the metallo-organic precursor and can be written as follows:

$$M-(OR)_n + H_2O \rightarrow HO\text{-}M-(OR)_{n-1} + R\text{-}OH \qquad (II.3)$$

It reveals reactive functions M-OH and is accompanied by the consumption of water and the release of a molecule of alcohol. The reaction is repeated on each OR group bonded to the metallic atom **[36]**.

- The Condensation:

The Condensation reaction is also a complex mechanism that occurs as soon as hydroxyl groups are formed. During condensation, two competitive mechanisms must be considered: alkoxolation and oxidation **[45]**.

❖ Alkoxolation:

Alkoxalation is a reaction in which an alcohol molecule is removed during condensation. This results in the formation of "oxo" bridges between two metal atoms (M-O-M) bond

$$(OR)_{n-1}-M-OR + OH-M-(OR)_{n-1} \rightarrow (OR)_{n-1}-M-O-M-(OR)_{n-1} + R\text{-}OH \qquad (II.4)$$

❖ The Oxolation:

This mechanism occurs between two partially hydrolyzed alcoholates. The mechanism remains the same, except that the leaving group is a molecule of water.

$$(OR)_{n-1}-M-OH + HO-M-(OR)_{n-1} \rightarrow (OR)_{n-1}-M-O-M-(OR)_{n-1} + H_2O \qquad (II.5)$$

When these two reactions are complete (Hydrolysis and Condensation), a gel is obtained **[46]**.

### II.2.5 : The Sol-Gel transition:

The changes in mechanical properties during the Sol-Gel transition are spectacular. The structure of the gel at this moment of transformation (freezing point) is very different from that of the network, It is described on a nanoscale and is defined as having a fractal geometry **[36]**. For a good interpretation of the phenomena related to the Sol-Gel transition, the scheme chosen for gelation is, generally, that of growing polymeric chains which are agglomerate by the condensation to form clusters. During the progress of the hydro-condensation reactions, polymeric clusters are generated, the size of which increases with the time. When one of these clusters reaches the infinite dimension, practically the size of the reaction vessel, the viscosity becomes infinitely similar: this is the Sol-Gel transition point. From this moment, the infinite cluster called "Frost Fraction" continues to grow by incorporating smaller polymeric groups. When all the bonds have been used, the gel is formed. From a macroscopic point of view, the transition can be followed by the mechanical behavior of the solution (viscosity and elasticity). If we follow the evolution of these viscoelastic properties of the solution as a function of time, we notice a divergence of the viscosity of the solution and an increase in the elastic constant (G) (or coulomb modulus) in the gel phase **[47]**. The evolution of the sol viscosity and that of its Coulomb modulus as a function of time are represented schematically in Figure (II.5).

At the complete formation of the gel, the viscosity becomes infinite, while the elastic constant tends towards its maximum value. The solid cluster formed from the basic solution can then be seen as an interleaving of the polymer chains forming a disordered solid structure. Structure still contains trapped liquid masses **[48]**. Their elimination is done by evaporation **[36]**.

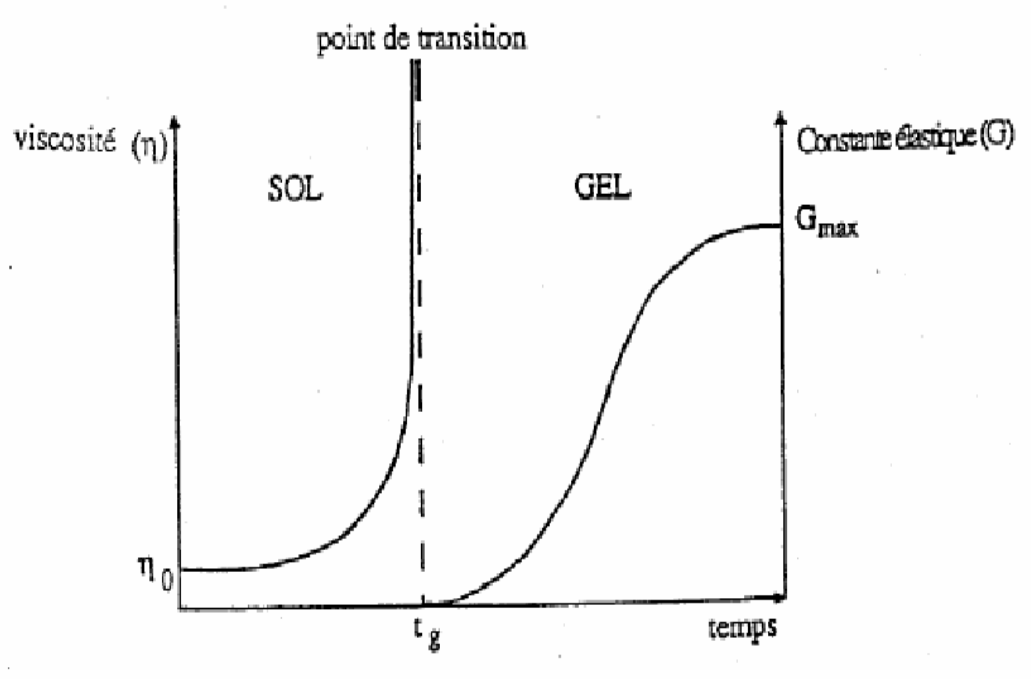


Figure II.5 : Evolution of the viscosity of the solution and the elastic constant of the Gel ; tg is the time after which the Sol-Gel transition is reached [36].

### II.2.6 : Heat treatment:

#### II.2.6.1 :Drying:

The drying is a low temperature heat treatment to evaporate the entrapped solvents in the structure of the wet gel and continue condensations between M-OH group present in the gel. There are several types of drying **[49]**, but two main ways (a and b) are mentioned below and defined in Figure (II.6):

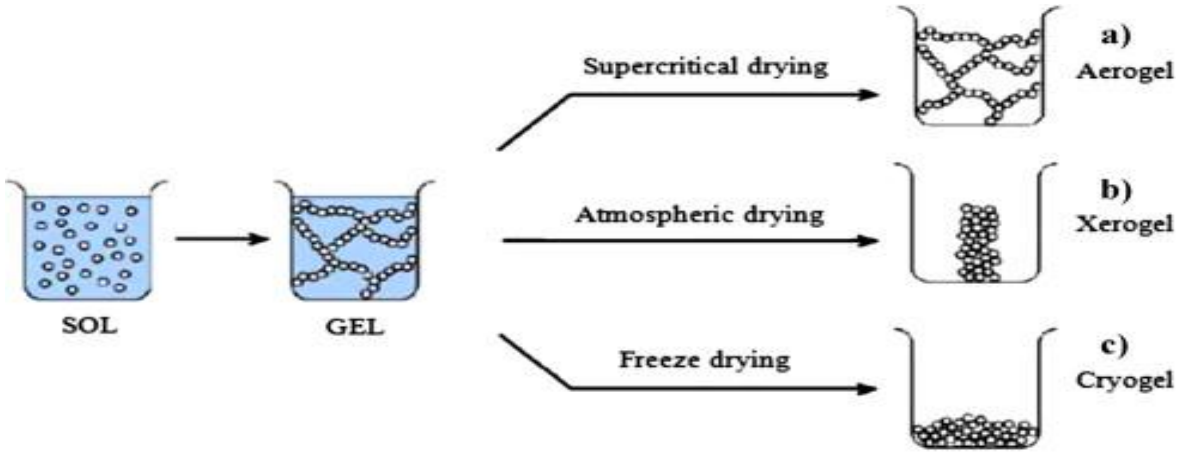


Figure II.6 : Methods of drying a wet gel to give an (a) Aerogel, (b) Xerogel and (c) Cryogel [50].

**a) Aerogel:**

It is a drying in critical conditions (in an autoclave under high pressure) causing little or no shrinkage of volume. The removal of the solvent under supercritical conditions leads to the formation of an aerogel that have not undergone any densification. wich gives a very porous material with exceptional properties. The passage from "Sol" to "Gel", whose viscosity can be controlled, also allows the production of fibers and films on various substrates by soaking or spraying **[15,51]**.

**b) Xerogel:**

On the contrary, xerogels are gels that are dried at a temperature close to ambient and at an atmospheric pressure. the volume of the dry material is generally much lower than the Sol-Gel volume of the wet gel **[49]**.

### II.2.6.2 : Annealing:

The heat treatment or annealing, is distinct from the drying phase; this phase is essential in the formation of the material. Annealing has three main functions: Elimination of the remaining organic matter present in the starting solution, crystallization of the species and densification of the material.

Indeed, after drying, the Alkyl groups (-OR) are always present in the film. It also allows the closing of pores. But all these changes are at the origin of the upheaval of the mechanical equilibrium leading to the creation of constraints. The anneals are generally carried out at temperatures between 300 °C and 1400 °C **[40]**.

## II.2.7 : Advantages and Disadvantages of Sol-Gel method:

### II.2.7.1 : The advantages:

The advantages of this method are manifold making it a coveted method; we quote here their main advantages:

- Simplicity of the process and speed of execution.
- Simultaneously coating both sides of the substrate in a single operation (dip-coating) and the ability to form multilayer.
- Ability to optimize the morphology of the films based on researched applications.

- Ability to produce thin films of inorganic oxides at low temperature on heat sensitive substrates.
- Possibility of making organo hybrid materials as thin or monolithic layers with specific properties **[4]**.

**II.2.7.2 : The disadvantages:**

The main disadvantages are:

- Cost of high - Alkoxide precursors.
- Manipulation of a large amount of solvents.
- The major drawback is the low thickness of the layers, so one must perform several steps of depositing and drying to obtain a thickness of several hundred nanometers, this increases the risk of cracking as the first deposited layers undergo all successive drying which increases the risk of short circuit when the electrical tests **[52]**.

## II.3 : Thin film characterization:

In order to find optimal experimental conditions for a specific purpose, feedback on the sample elemental composition, phases present, crystal orientation, crystal quality, physical properties, etc. is needed. In this work, the following thin film characterization techniques have been used **[53]**.

### II.3.1 : X-Ray diffraction:

X-Ray diffraction (XRD) is a simple and non-destructive analysis technique which provides means to identify different phases and their distribution in the sample, texture, evaluate average grain size, internal stress, etc.

X-Rays are electromagnetic waves with wavelength (0.5-50 Å) comparable to atomic separation distances. When propagating through a crystal, the X-Rays interact with the lattice and are diffracted according to the Bragg's law:

$$\boldsymbol{n\,\lambda = 2\,d\,sin\theta} \qquad \text{(II.6)}$$

where $d$ is the atomic spacing, $\theta$ is the scattering angle, $n$ is an integer number, and $\lambda$ is the wavelength **[53]**.

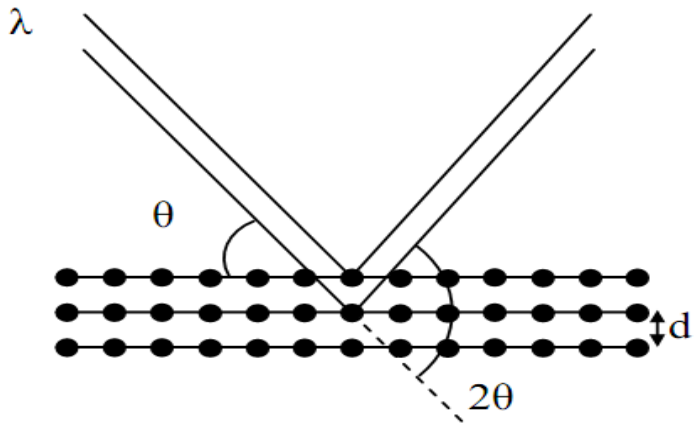


Figure II.7 : Schematic illustration of an XRD θ/2θ measurement [53].

X-Ray Diffraction measures the average spacing between the layers or row of the atoms, finds the crystal structure of unknown materials. In addition to that determines the orientation of single crystal or grain. It can analyze The different phases and we can also get all the crystal parameters from the X-Ray data by using the software **[54]**.

### II.3.1.1 : Determination of the Grains size:

The average grain size of the film can be calculated by using the Scherrer's formula **[4]**.

$$D = \frac{0.9\lambda}{\beta cos\,\theta} \qquad \text{(II.7)}$$

Where , $D$ : The average size of crystallites expressed in (nm).

$\lambda$ ：the wavelength of the X-Ray.

$\beta$ : The full width at half maximum intensity of peak in (rad).

$\theta$: The angle of the diffraction peak (rad).

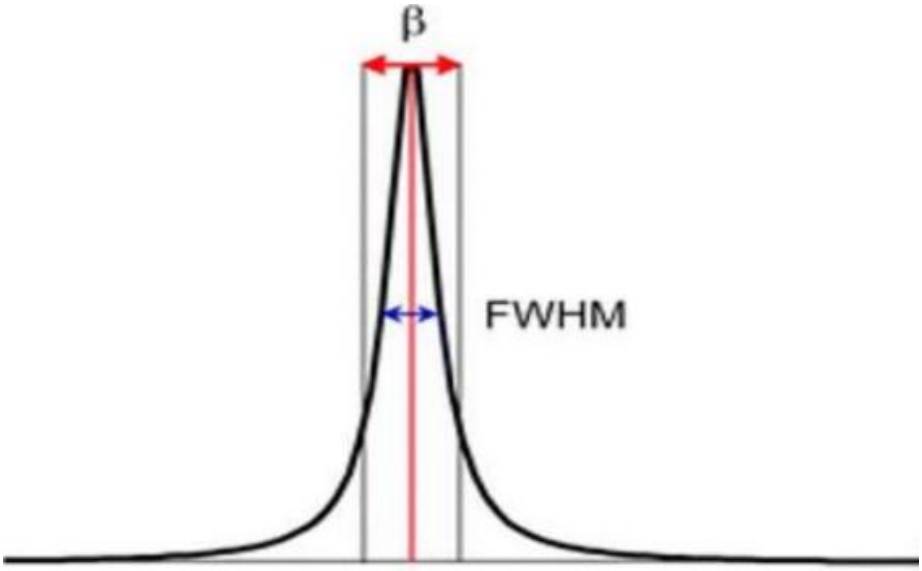


Figure II.8 : Illustrate the peak widths FWHM [49].

### II.3.1.2 : Determination the Dislocation density:

From the grain size, the dislocation density $\delta$ can be calculated using the following relation **[55]**

$$\delta = \frac{1}{D^2} \qquad \text{(II.8)}$$

Where, $D$ : The average size of crystallites expressed in (nm).

### II.3.1.3 : Determination of the Deformation:

To calculate the deformation using the following relation **[26]** :

$$\varepsilon = \frac{\beta \cos\theta}{4} \qquad \text{(II.9)}$$

Where, $\beta$ : The full width at half maximum intensity of peak in (rad).

$\theta$: The angle of the diffraction peak (rad).

## II.3.2 : Spectroscopy (UV-VISIBLE):

The domains of spectroscopy are generally distinguished according to the interval of the wavelength in which the measurements are made. We can distinguish the domains: visible ultraviolet, infrared.

In our case, we used a dual-beam recording spectrophotometer, whose operating principle is shown in Figure (II.9), by which we could plot curves representing the variation of the transmittance, as a function of the wavelength in the domain UV-visible and near-infrared. By exploiting these curves, it is possible to calculate the thickness of the films and determine its optical characteristics; Optical absorption threshold, absorption coefficient, band gap width, Urbach energy, and refractive index **[40,49]**.

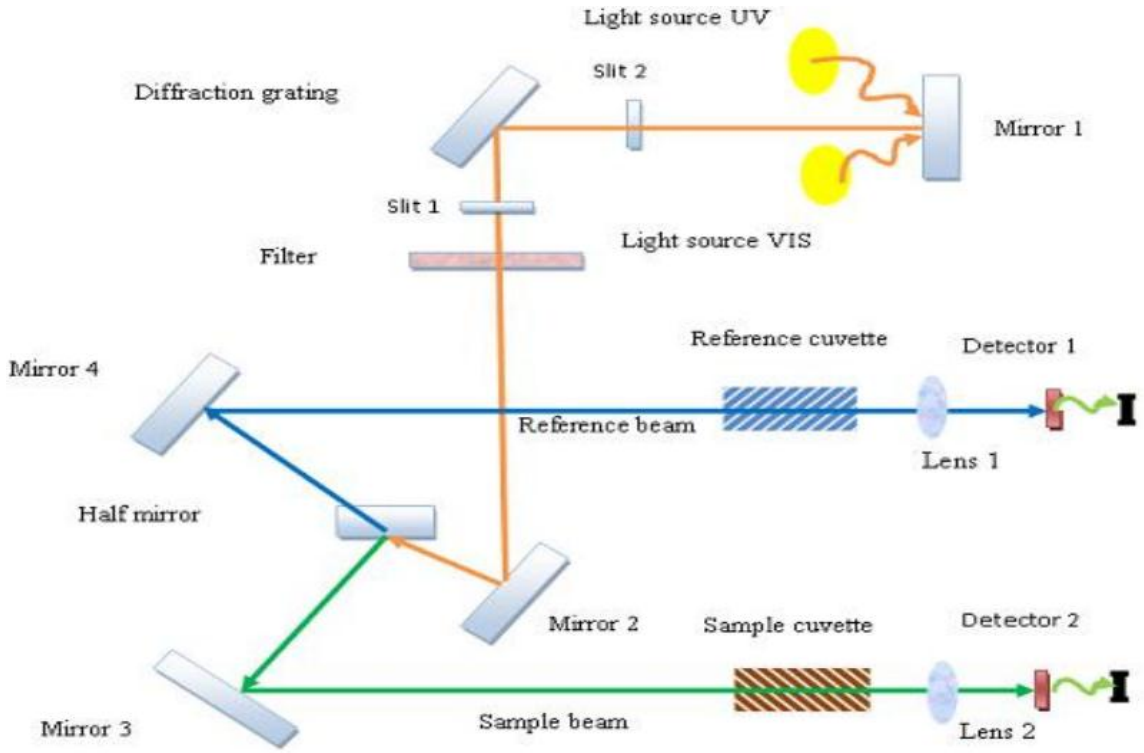


Figure II.9 : The principle of operation of UV-Visible [4].

### II.3.2.1 : The thickness of the film:

We used two methods to measure the thickness of our samples:

#### a) Interference fringe method:

Using the physical parameters that are defined in the figure and the transmission spectra obtained, we can determine the thickness of the film as follows **[56]**.

$$d = \frac{\lambda_1 \lambda_2}{2(\lambda_2 n_1 - \lambda_1 n_2)} \quad \text{(II.10)}$$

Where : $n_1$ and $n_2$ are the refraction index of the film for the wavelength $\lambda_1$ and $\lambda_2$.

We can calculate $n_1$ and $n_2$ from the following relation:

$$n_{1,2} = \left[ N_{1,2} + \left( N_{1,2}^2 - s^2 \right)^{1/2} \right]^{1/2} \quad \text{(II.11)}$$

And $N_{1,2}$ can be obtained using this relation:

$$N_{1,2} = 2s.\frac{(T_M - T_m)}{T_M.T_m} + \frac{s^2+1}{2} \quad \text{(II.12)}$$

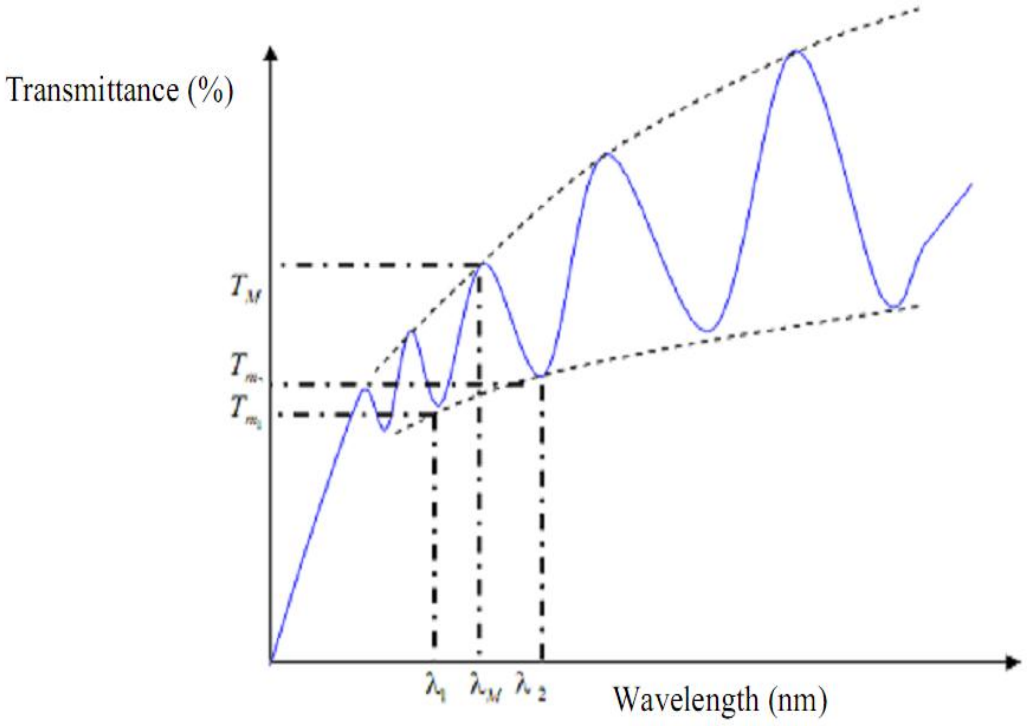


:

Figure II.10 : Method of interference fringes to determinate the thickness[4].

**b) Gravimetric method:**

The thickness "$d$" is calculated using the gravimetric method **[57]**.

$$d = \frac{\Delta m}{\rho . s} \quad \text{(II.13)}$$

Where, $\Delta m$ : the mass of the deposited layer (g).

$S$ : the surface of the sample ($cm^2$).

$\rho$ : the density of the layer ($g/cm^3$).

**II.3.2.2 : Optical Gap:**

In a high energy, absorption results from electronic transitions between wide states of the band to band. It is usually described by Tauc law:

$$(\alpha h\nu)^n = A(h\nu - E_g) \quad \text{(II.14)}$$

Where: $h\nu$ is the photon energy, $E_g$ is optical gap $n$ and A are constants, $n$ characterizes the optical type of transition and takes the values $1/2$ or 2 ($1/2$ for allowed direct transitions or 2 for allowed indirect transitions). In order to determine the nature of the transition from films produced in this study, we will plot the curves $(\alpha h\nu)^2 = f(h\nu)$ **[58]**.

We can obtain $E_g$ value as is shown in figure (II.11):

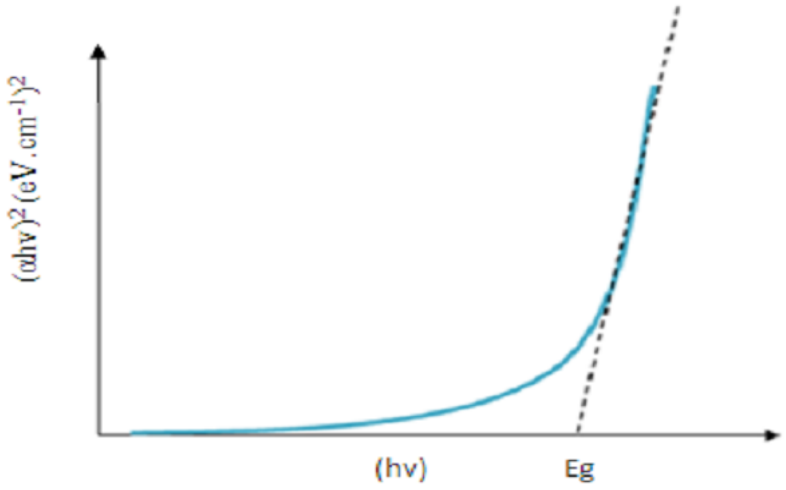


Figure II.11 : Determination of $E_g$ [5].

### II.3.2.3 : Urbach energy:

Another important parameter which characterizes the material disorder is Urbach energy, According to the Urbach law of the expression of the absorption coefficient is as follow:

$$\alpha = \alpha_0 . \exp\left(\frac{h\nu}{E_u}\right) \quad \text{(II.15)}$$

Where, $\alpha_0$: is constant.

$E_u$ : Urbach energy .

By drawing the $ln\ (\alpha)$ as a function of $h\nu$, one can determinate $E_u$value:

$$ln\ (\alpha) = ln\ \alpha_0 + \frac{h\nu}{E_u} \quad \text{(II.16)}$$

The following figure presents how we can estimate $E_u$ **[4]**.

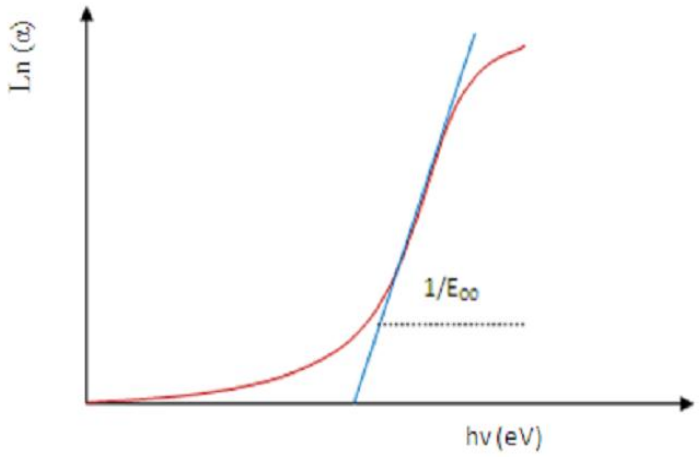


Figure II.12 : Determination of the disorder by extrapolation starting from the variation of $ln(\alpha)$ has in function of $h\nu$ [5].

## II.3.3 : Scanning Electron Microscopy (SEM):

The scanning Electron Microscope is an electron microscope which produces images of a sample by scanning it with a focused beam of electrons. The angular resolution of optical microscopes is limited by the wavelength of the visible spectra. Replacing of photons by electrons, which have a lower wavelength, allows achieving the resolution down to 0.4nm.

The electron beam generated by an electron gun is focused on the sample. Primary electrons interact with the sample material and generate secondary electrons, X-ray radiation,

Auger electrons, which can be detected by special detectors. The intensity of these signals strongly depends on the topography of the tested material.

The main types of signals that generated and detected during the operation of SEM:

- Secondary electrons.
- Reflected electrons.
- Electrons passed through the sample.
- Electron backscatter diffraction.
- X-Ray radiation**[9]**.

## II.3.4 : Four-point probe method:

It is a simple and fast method that measures the resistivity of thin layers. It is based on the use of equidistant fourth points (probes) in direct contact with the surface of the sample, placed either linearly or in the form of a square (FigII.13). The principle of the measurement is simple, it is enough to inject a current (I) to the two extreme points and to measure the tension (V) at the two internal points **[59]**.

When the distance $\boldsymbol{a}$ between the terminals is much greater than the thickness of the thin film, i.e. $\boldsymbol{d} << \boldsymbol{a}$ (the thickness is negligible compared to other dimensions), the lateral dimensions can be considered infinite. In this case, a two-dimensional model of conduction is considered "$a$ cylindrical propagation of field lines in the thin layer" and gives **[60]**:

$$\frac{\boldsymbol{U}}{\boldsymbol{I}} = \boldsymbol{K}.\frac{\boldsymbol{\rho}}{\boldsymbol{d}} \qquad \text{(II.17)}$$

With : $\rho$ : the resistivity of the layer.

$d$ : thickness.

$K$ : coefficient ($K = \frac{ln2}{\pi}$).

The report $\frac{\boldsymbol{\rho}}{\boldsymbol{d}}$ characterizing the l ayer is noted $R_S$ and is expressed in $\Omega$.

At an available *K* coefficient, $R_S$ is the ratio between the voltage U and the current I. According to the preceding observations, we have the formula to deduce the resistivity of the four-point measurement knowing the thickness:

$$\rho = \left(\frac{\pi.U}{ln2\ .I}\right).d = R_s.d \qquad \text{(II.18)}$$

And their conductivity is:

$$\boldsymbol{\sigma = \frac{1}{\rho}} \qquad \text{(II.19)}$$

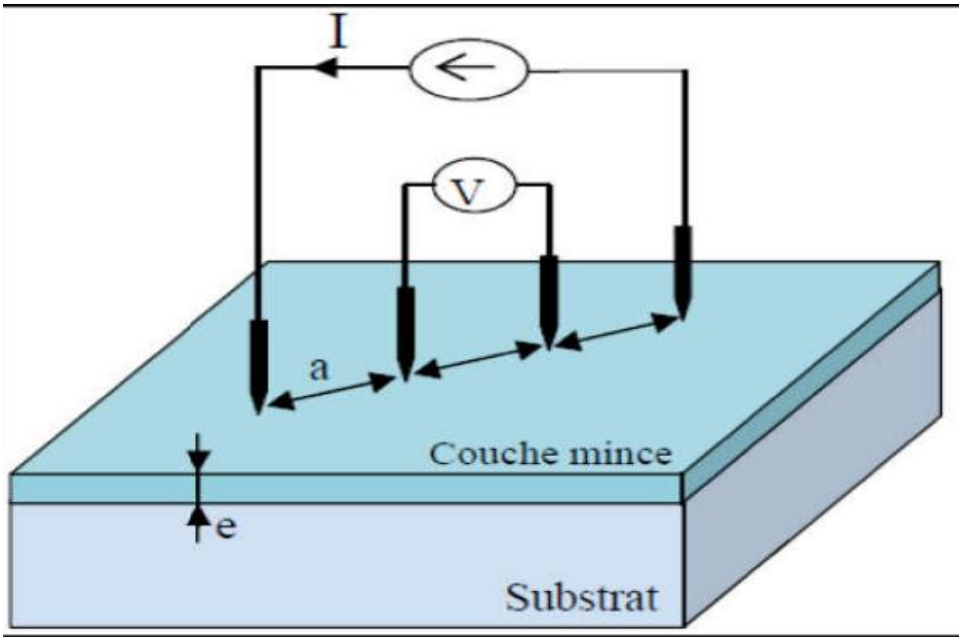


Figure II.13 : Diagram of a device four points aligned [49].

# Chapter3:

# Experimental procedures, Results and discussions

In this chapter, we presente the results of our work concerning the elaboration and characterization of undoped Titanium Dioxide films and doped with nuibium ($TiO_2$: Nb) deposited by the method of spin coating. Then, we will analyze the obtained results. The influence of Nb doping concentration on the structural, optical and electrical properties of $TiO_2$ was studied.

## III.1Experimental procedures :

### III.1.1Preparation of the solution:

In all samples, the starting solution (0.2 mol / L) contains 0.601 ml of Titanium Tetraisopropoxide (TTIP) used as a precursor are dissolved in 10 ml of ethanol and 0.207ml of acetylacetone, with a certain percentage of niobium chloride (V) $Nbcl_5$ as a source of doping source. The mixture is stirred by a magnetic stirrer at 50 ° C for 3 hours. The molar ratio of acetylacetone (stabilizer) and TTIP is equal to 1. The final solution is transparent yellowish and slightly viscous. We present the different physico-chemical properties of the used elements used for the preparation of our samples.

- ***Titanium Tetra-Isopropoxide (precursor) :***


**Synonym:** Titanium (IV) isopropoxide.
**Appearance:** Colorless to light yellow liquid.
**Molar mass:** 284.23 g / mol.
**Density:** 0.955 g / $cm^3$.
**Purity:** 95%.
**Solubility:** Soluble in ethanol.
**Boiling temperature:** 232 °C.

- ***Acetylacetone (catalyst) :***


**Formula:** $C_5H_8O_2$.
**Appearance:** Transparent liquid.
**Molar mass:** 100.12 g / mol.
**Density:** 0.97 g / cm3 at 20 °C.
**Purity:** 99.5%.
**Boiling point:** 140.4 °C.

- ***Ethanol (solvent) :***

**Synonym:** Ethyl alcohol.

**Formula:** $C_2H_5OH$.

**Appearance:** Transparent liquid.

**Molar mass:** 46.07 g / mol.

**Density:** 0.789 g / $cm^3$ at 20 °C.

**Boiling temperature:** 78.37 °C.

- ***Niobium chloride (dopant):***

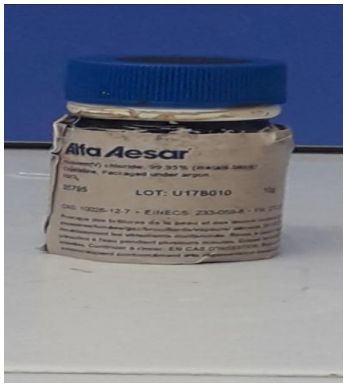


**Synonym:** Niobium chloride (V).

**Formula:** $Nbcl_5$.

**Molar mass:** 270,17 g/mol.

**Density:** 2.74 g / $cm^3$.

**Purity:** 99.95%.

**Boiling temperature:** 248.2 °C.

### III.1.2: Preparation of the substrate:

#### III.1.2.1: Choice of the substrate:

In this work, we choose the glass slide as a substrate, for the following reasons:

1. For their transparency which adapts well for the optical characterization of films in the visible one **[4]**.
2. The softening temperature of the glass is higher than the temperature of the heat treatment that our films have undergone after deposition, and its coefficient of thermal expansion is compatible with that of the deposited material which serves to limit the effects of stresses during annealing **[13]**.
3. The glass substrate is insulating which allows a good electrical characterization of our films.
4. For economic reasons.

### III.1.2.2: Cleaning of the substrate:

The adherence and the quality of thin films repose on purity and the state of substrate thus the cleaning of the substrate is one of the most important steps for getting a good result. The surface of each substrate must be cleaned to remove the various contaminants that cover it (grease, dust, fingerprints, organic impurities, etc.) .The cleaning of our substrates surfaces is as follows:

- The substrates are cut using a pen with a diamond point.
- Rinsing with distilled water.
- Cleaning with acetone for 5 min.
- Rinsing with distilled water.
- Cleaning with ethanol for 5 min.
- Rinsing with the distilled water.
- Drying using a drier.

### III.1.3: Depositing of thin films:

The deposition procedure comes right after the preparation of the substrates and the solution. In our work, we used a machine called "Holmarc spin coater".

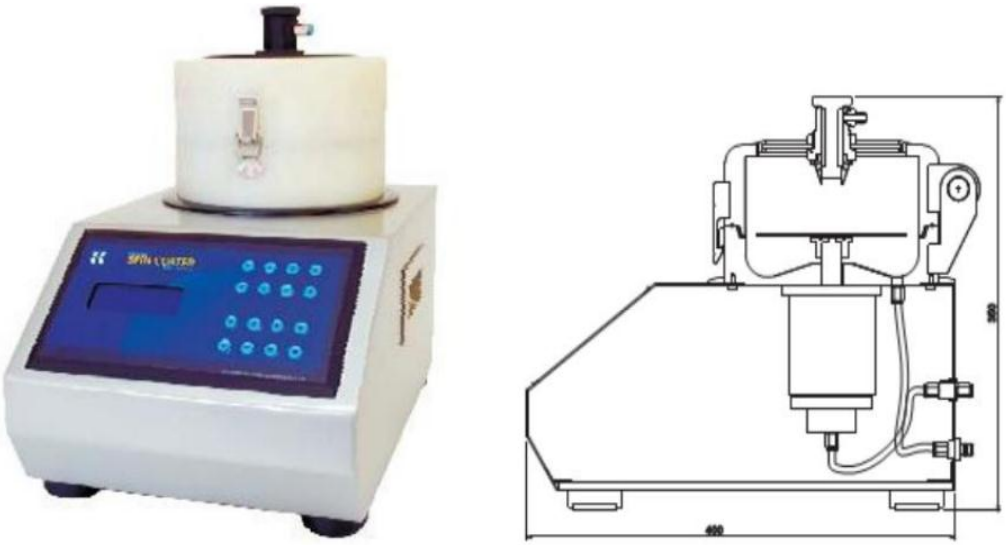

Figure III.1 : Holmarc Spin coater.

### III.1.3.1: Experimental conditions:

The experimental conditions of elaborations of our $TiO_2$ layers doped with Niobium represented on the following table :

Table III.1 : The experimental conditions.

| Solution | TTIP + Ethanol + Acetylacetone +concentration of dopant ($Nbcl_5$) | | | | | |
|---|---|---|---|---|---|---|
| Molarity (mol / l) | 0,2 | | | | | |
| Volume of the solution (ml) | 10 | | | | | |
| Rotation speed (rpm) | 4000 | | | | | |
| Acceleration (rpm) | 400 | | | | | |
| Filing time (s) | 30 | | | | | |
| Drying temperature (°C) | 250 | | | | | |
| Drying time (min) | 10 | | | | | |
| Annealing temperature (°C) | 600 | | | | | |
| Annealing time (h) | 2 | | | | | |
| Number of repetition (spin + drying) | 5 fois | | | | | |
| Percentage of doping (Nb at%) | 0 | 2 | 4 | 6 | 8 | 10 |

Firstly, a small amount of ~ 250 µl of the solution is withdrawn with the aid of a syringe. Then it is deposited on the substrate mounted on the spinor support which is then rotated by a constant rotational speed.

The deposition step is followed by two other thermal operations essential for densification of thin films: drying and annealing. They are necessary for obtaining thin films of good quality.

## III.1.4: Heat treatment:

### III.1.4.1: Drying of thin films:

Once deposited, the thin films have been dried at 250 °C for 10 minutes, in order to eliminate almost all the solvent and to jellify the layer. Drying is a very important step in producing good quality materials; it corresponds to the evaporation of the residual solvents by diffusion through the pores.

This process repeated 5 times for obtaining a final film.

### III.1.4.2: Annealing of thin films:

The final densification is obtained after annealing in a resistance furnace for 2 hours in air, and at a fixed temperature of 600 °C. It is only after this annealing that the desired material can be obtained.


Figure III.2 : Annealing furnace.

The procedure for thin films deposition by sol-gel (spin-coating) is illustrated in the following diagram:

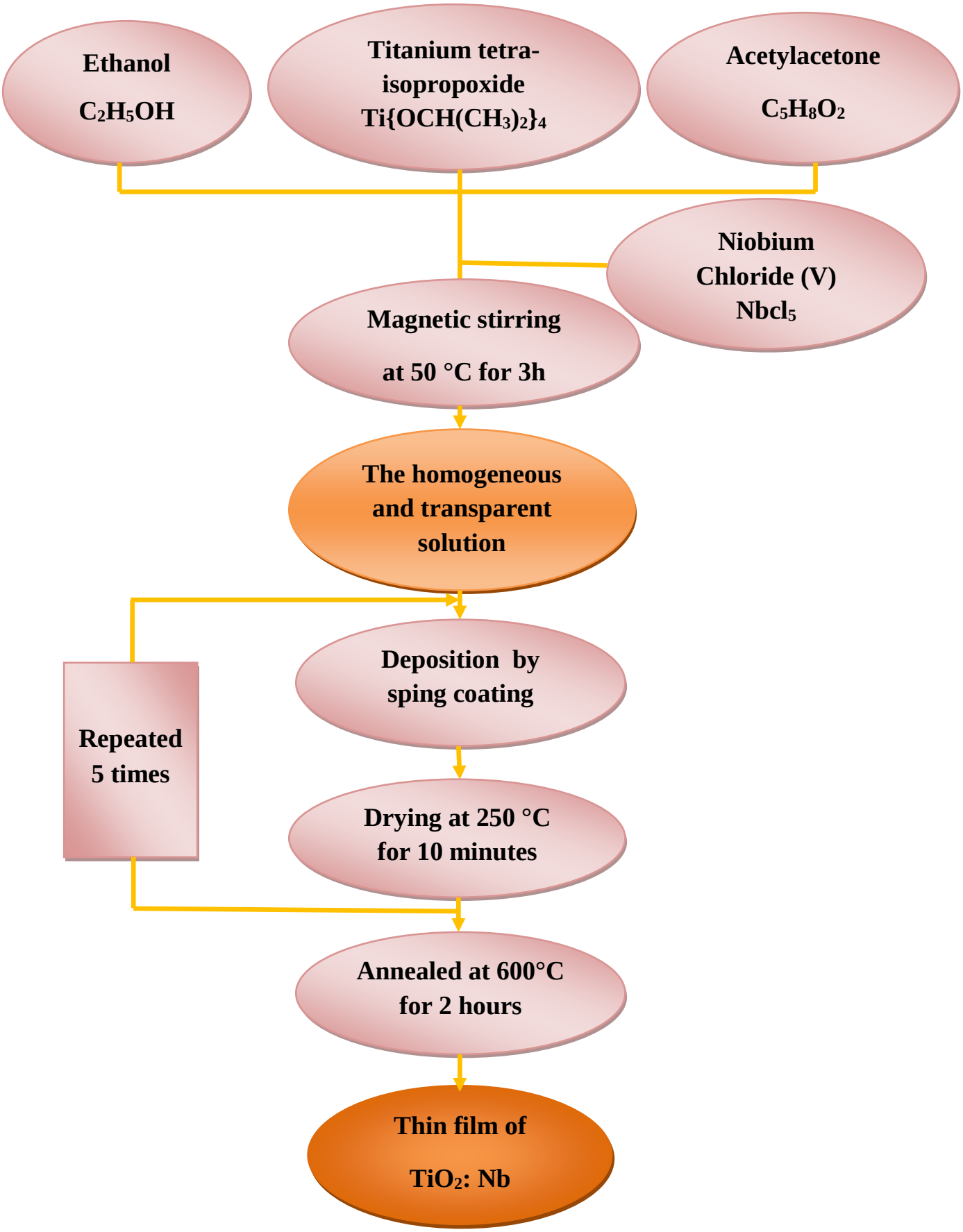


Figure III.3 : Diagram showing the deposition steps of $TiO_2$: Nb thin films.

## III.2 : Results and discussions :

In our calculations, we have followed methods mentioned in the second chapter.

### III.2.1 : Adhesion test:

The term ‘’ Adhesion’’ refers to the interaction between the closely contiguous surfaces of adjacent bodies, i.e., a film and substrate. According to the American Society for Testing and Materials (ASTM), ‘’Adhesion’’ is defined as the condition in which two surfaces are held together by valence forces, by mechanical anchoring, or by both together. Adhesion to the substrate is certainly the first attribute a film must possess before any of its other properties can be manifested or exploited. The simplest and quickest qualitative measure of film or coating adhesion is Tape Test which consists of :

An adhesive tape is applied to the film surface and pulled off again. The tape test is a subjective test which is not only dependent on the type of tape but also on the pull off velocity and the pull off angle **[61]**.

For our ($TiO_2$:Nb) thin films, we observed no delaminated either completely neither partially so we can say that the adhesion was not bad according to make the test above.

### III.2.2: The thickness of the film:

We calculate the film thickness using the method of interference fringes which was mentioned in the second chapter , the obtained results are represented in the table below :

Table III.2 : The thickness of ($TiO_2$: Nb) thin films deposited at different concentration.

| Nb (at%) | d (nm) |
|---|---|
| 0% | 644,99 |
| 2% | 440,58 |
| 4% | 300,51 |
| 6% | 493,74 |
| 8% | 547,26 |
| 10% | 554,77 |

We present the variations of the thickness of our films in the following figure:

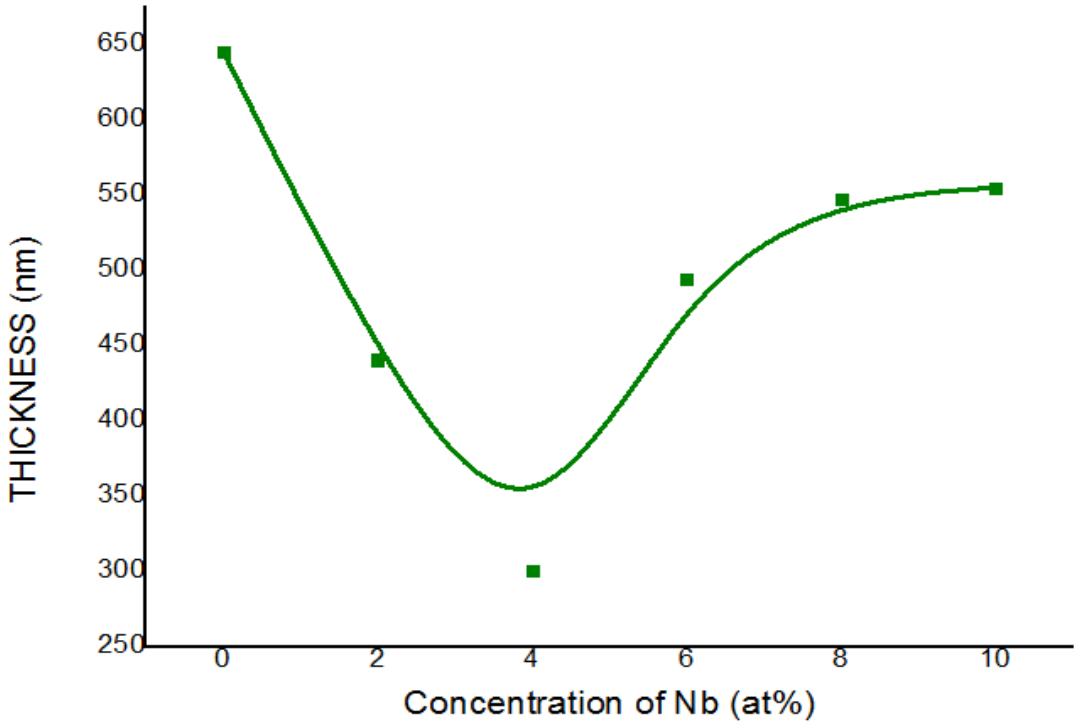


Figure III.4 : The variations of the thickness as a function of the doping rate.

From figure (III.4), we can observed that the thickness of $TiO_2$ decreases as doping increases, until 4% thereafter , it starts to increase.

We can explain the variation of film thickness as a function of doping concentration as follows: 0% Nb (undoped), the film thickness has a higher value compared to other samples. This is physically reasonable. It can be explain as follow ; annealing temperature sufficient for a move of $TiO_2$ nanoparticle, but with increasing of Nb doping concentration the kineticl energy of $TiO_2$: Nb nanoparticles decrease **[5]**.

## III.2.3 : Structural characterization:

### III.2.3.1 : X.Ray diffraction:

To study the structural properties of thin layers of Niobium-doped $TiO_2$ produced by the Sol-Gel method, we used X-Ray diffraction of the Mini-Flex type (RigaKu) (thin films laboratory -Biskra), which allowed us to have the diffractograms of Niobium-doped $TiO_2$

films from its spectra, we can determine the crystallinity, the nature of the phases present as well as the (hkl) planes.

The different peaks characteristic of the $TiO_2$ structure for different concentrations of Niobium are grouped together in figure (III.4) :

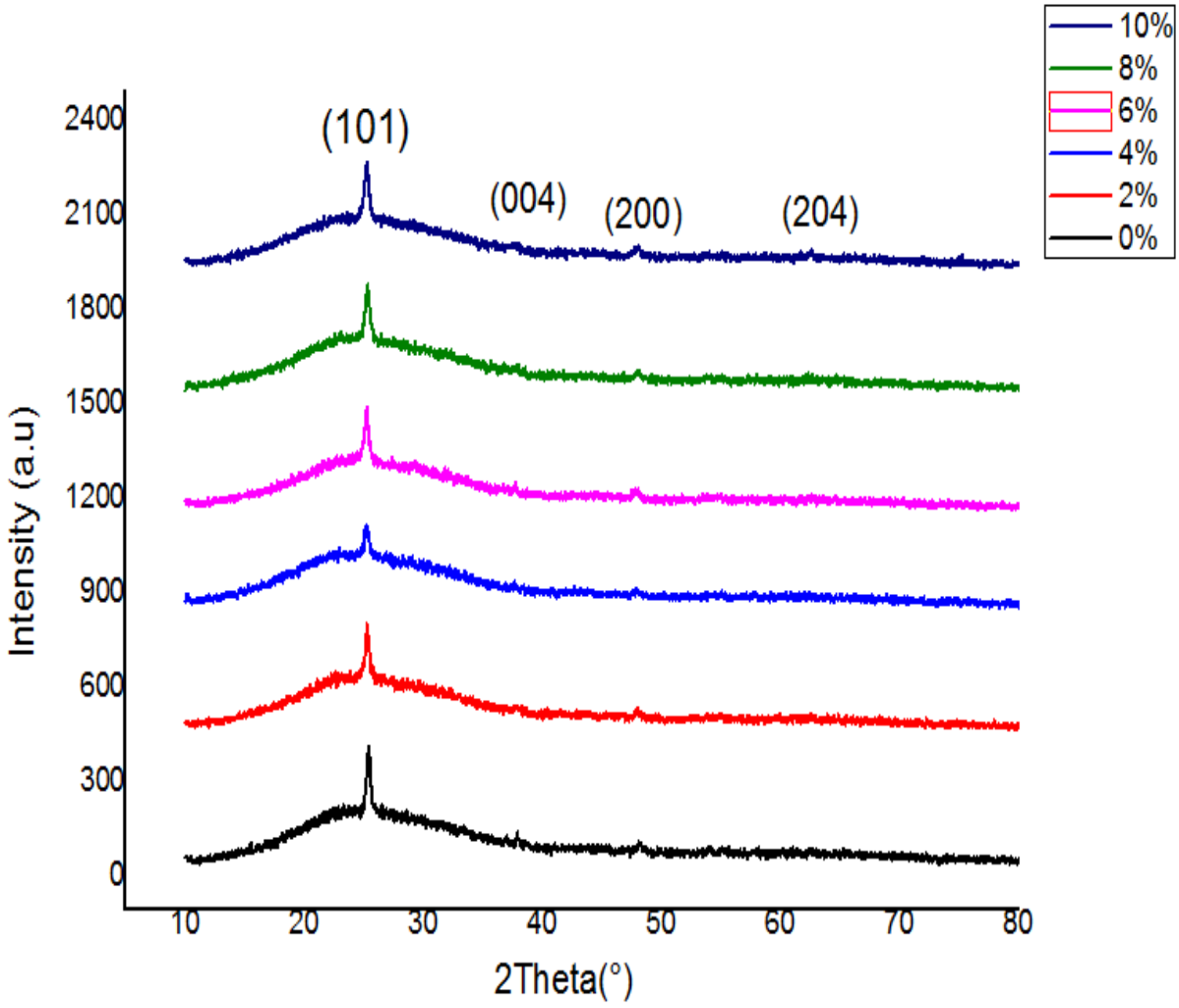


Figure III.4 : X-Ray diffraction patterns for Nb-doped $TiO_2$ thin films

To obtain the Miller indices of our layer planes, we used the ASTM sheet of Titanium Oxide shown in the following figure (III.5) :

29-1360 Wavelength= 1.54056

TiO2

Titanium Oxide

Brookite

Rad.: CuKa1 λ: 1.54056 Filter: Ni Beta d-sp:

Cut off: Int.: Diffract. I/Icor.:

Ref: Natl. Bur. Stand. (U.S.) Monogr. 25, 3, 57 (1964)

Sys.: Orthorhombic S.G.: Pcab (61)

a: 5.4558 b: 9.1819 c: 5.1429 A: 0.5942 C: 0.5601

α: β: γ: Z: 8 mp:

Ref: Ibid.

Dx: 4.120 Dm: 4.140 SS/FOM: $F_{30}$ = 58(.0116 , 45)

εα: 2.5831 ηωβ: 2.5843 εγ: 2.7004 Sign: + 2V: ~25°

Ref: Dana's System of Mineralogy, 7th Ed., I, 588 (1944)

Color: Black

Pattern taken at 25 C. Specimen from Magnet Cove, AR, USA (USNM 97661). Spectrographic analysis: 0.1-1.0% Si; 0.01-0.1% each of Al, Fe, and V; 0.001-0.01% Mg. Niobian brookite from Mozambique [Chemical analysis (wt.%): Ti 02 80.7, Nb2 05 14.1, FeO 5.53]; Carvalho et al., Rev. Cien. Geol. Ser. A, 7 61 (1974) reports an identical pattern. Intensities verified by calculated pattern. 02 Ti type. PSC: oP24. To replace 16-617 and validated by calculated pattern. Mwt: 79.90. Volume[CD]: 257.63.

| 2θ | Int | h | k | l | 2θ | Int | h | k | l |
|---|---|---|---|---|---|---|---|---|---|
| 25.339 | 100 | 1 | 2 | 0 | 71.488 | 3 | 4 | 0 | 1 |
| 25.689 | 80 | 1 | 1 | 1 | 71.929 | 2 | 2 | 3 | 3 |
| 30.807 | 90 | 1 | 2 | 1 | 73.646 | 2 | 0 | 0 | 4 |
| 32.790 | 4 | 2 | 0 | 0 | 76.946 | 10 | 0 | 2 | 4 |
| 36.251 | 25 | 0 | 1 | 2 | 79.022 | 2 | 4 | 3 | 1 |
| 37.296 | 18 | 2 | 0 | 1 | 79.281 | 1 | 1 | 2 | 4 |
| 37.933 | 6 | 1 | 3 | 1 | 83.640 | 4 | 3 | 3 | 3 |
| 38.370 | 4 | 2 | 2 | 0 | 84.285 | 2 | 0 | 8 | 0 |
| 38.575 | 4 | 2 | 1 | 1 | 84.721 | 2 | 4 | 4 | 1 |
| 39.204 | 5 | 0 | 4 | 0 | 86.740 | 4 | 0 | 4 | 4 |
| 39.966 | 8 | 1 | 1 | 2 | 95.586 | 3 | 5 | 2 | 1 |
| 40.151 | 18 | 0 | 2 | 2 | 95.586 | 3 | 4 | 2 | 3 |
| 42.339 | 16 | 2 | 2 | 1 | 95.989 | 2 | 2 | 8 | 1 |
| 46.071 | 16 | 0 | 3 | 2 | 97.606 | 4 | 3 | 2 | 4 |
| 48.011 | 30 | 2 | 3 | 1 | 102.556 | 2 | 1 | 2 | 5 |
| 49.171 | 18 | 1 | 3 | 2 | 103.198 | 4 | 3 | 7 | 2 |
| 49.692 | 3 | 2 | 1 | 2 | 103.198 | 4 | 2 | 5 | 4 |
| 52.011 | 3 | 2 | 4 | 0 | | | | | |
| 54.203 | 20 | 3 | 2 | 0 | | | | | |
| 55.233 | 30 | 2 | 4 | 1 | | | | | |
| 55.710 | 5 | 1 | 5 | 1 | | | | | |
| 57.174 | 13 | 1 | 1 | 3 | | | | | |
| 57.683 | 2 | 2 | 3 | 2 | | | | | |
| 59.990 | 7 | 1 | 2 | 3 | | | | | |
| 62.064 | 10 | 0 | 5 | 2 | | | | | |
| 63.063 | 4 | 1 | 6 | 0 | | | | | |
| 63.414 | 9 | 3 | 1 | 2 | | | | | |
| 63.642 | 12 | 2 | 5 | 1 | | | | | |
| 64.103 | 12 | 2 | 0 | 3 | | | | | |
| 64.601 | 6 | 1 | 3 | 3 | | | | | |
| 65.001 | 10 | 2 | 1 | 3 | | | | | |
| 65.874 | 9 | 1 | 6 | 1 | | | | | |
| 68.766 | 5 | 4 | 0 | 0 | | | | | |
| 70.430 | 8 | 3 | 3 | 2 | | | | | |



Figure III.5 : ASTM Sheet (n° 29-1360) of $TiO_2$.

By comparing our X-Ray spectra with the ASTM sheet (n° 29.1360) which is shown in Figure (III.5), we observe several of the planes, this proves that the thin films of $TiO_2$ prepared are polycrystalline, these lines correspond to the anatase phase (tetragonal structure), with a preferential orientation according to the plane (101) **[62]**.

According to the figure (III.4), we observe a maximum intensity according to the plane (101), with the existence of other secondary peaks according to (004), (204) and (002) which correspond to the phase anatase **[63,64]**.

The presence of these orientations in the DRX spectra shows that there is a large possible direction for the growth of $TiO_2$ crystals. but it should be noted that our films are preferentially oriented according to the plane (101) and this is logical because of this plane of lower surface energy, this is attributed to the highest atomic density which reaches along the direction (100) **[65]**.

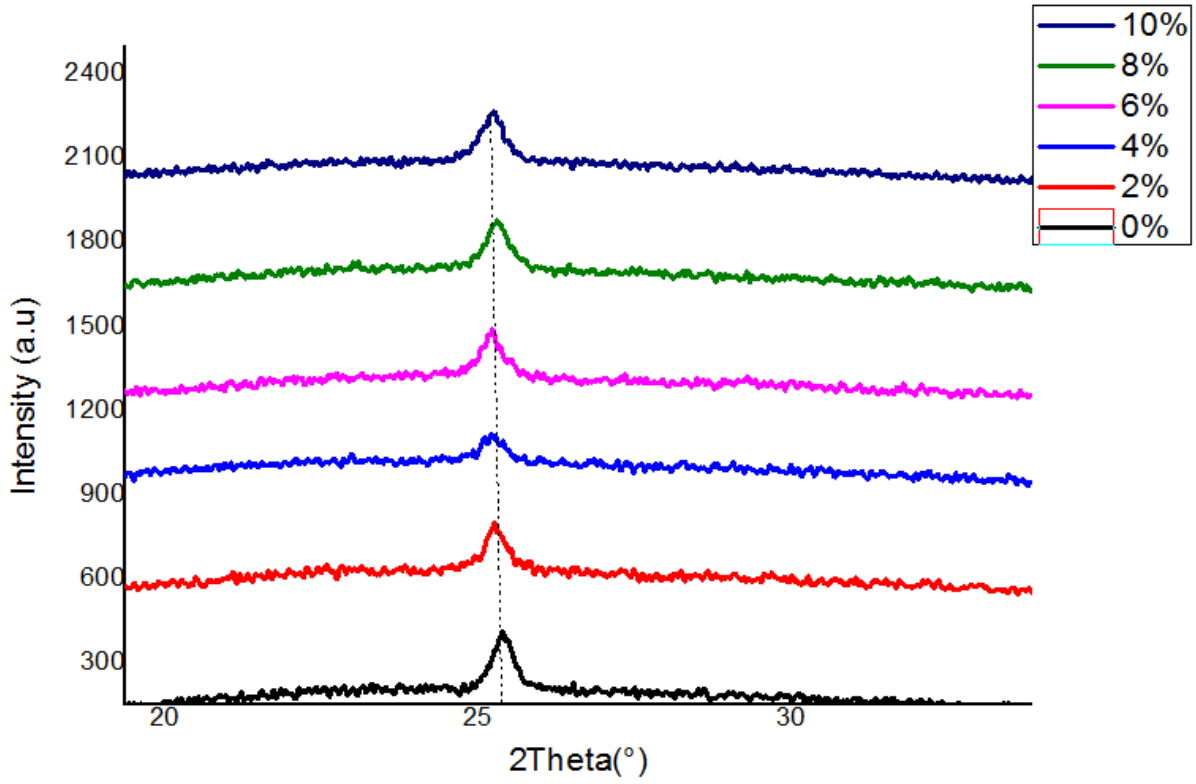


Figure III.6 : Peak position (101) with different Nb concentrations.

We observe that The (101) peak position moves slightly towards lower diffraction angle with Nb doping concentrations increasing as depicted in Fig. Based on Bragg formula $2d.\sin\theta = \lambda$, the interplanar spacing $d$ of (101) peak increases gradually as the corresponding diffraction angle θ decreases. The reason can be attributed to the fact that the radium of $Nb^{5+}$ ion (0.064nm) is larger than that of $Ti^{4+}$ ion (0.061nm) **[38]**. The doped $Nb^{5+}$ ions would put stress on the lattice and lead to distortion. Therefore, the lower shift of the (101) diffraction peak position partially indicates that Nb atoms have been doped in the lattice and substituted Ti atoms **[66]**.

### III.2.3.2 : Grains size and Deformation :

The grain size and deformation of the various $TiO_2$ films were calculated from the highest peak, using the relation (II.7, II.9) and the results are shown in the table (III.3), and illustrated in the figure ( III.7) :

Table III.3 : The Variation of grain size and deformation according to doping.

| Nb (at%) | Grains size (nm) | Strain ε |
|---|---|---|
| 0% | 16,724 | 0,109 |
| 2% | 13,325 | 0,138 |
| 4% | 11,854 | 0,155 |
| 6% | 12,711 | 0,144 |
| 8% | 13,752 | 0,133 |
| 10% | 13,917 | 0,132 |

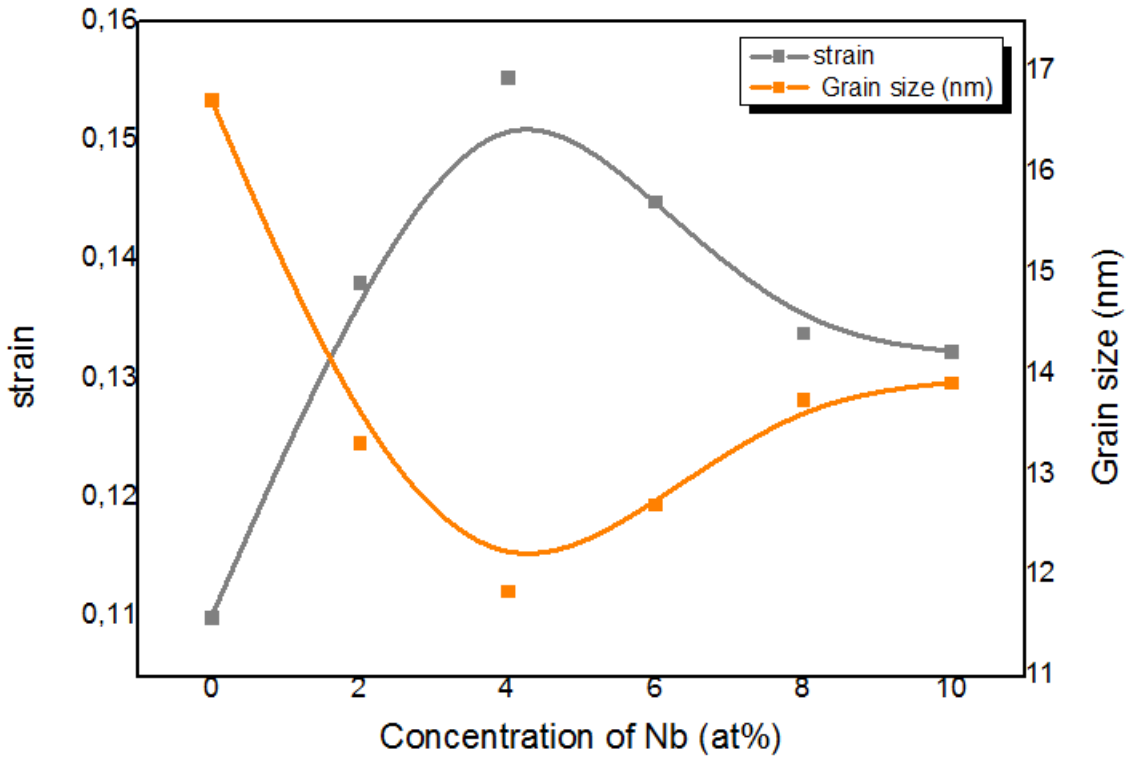


Figure III.7 : The variation of the grain size and the deformation of thin films of Nb-doped $TiO_2$.

From Figure (III.7), we can divide the grain size study of variation into two intervals:

- In the range of 0% to 4% the size of the grains is reduced with the increase in the percentage of doping, this reduction can be explained as follows: the ion $Nb^{+5}$ which has an ionic radius ($R_{Nb}$ = 0.064nm) plus large relative to the $Ti^{+4}$ Titanium ion ($R_{Ti}$ = 0.061nm) occupies the Titanium substitution sites **[67]**. Another explanation for the decrease in grain size due to increase in the density of nucleation sites **[68]**. This decrease gives an increased deformation due to the increase of grain boundaries.
- In the range of 4% to 10% the increase in grain size can be explained by the saturation of the substitution sites and the excess of Niobium that occupies the interstitial sites in the structure. From 4%, up to 10%, it is noted in this interval that the increase of grain size with doping leads to a decrease in the grain boundaries, while decreasing the density of the deformation **[69]**.

## III.2.4 : The Optical properties:

### III.2.4.1: Transmittance spectra:

The optical characterization of our thin films of $TiO_2$: Nb has been done is obtained using a UV-visible spectrophotometer. The transmittance spectra of our samples are illustrated in the figure (III.8) :

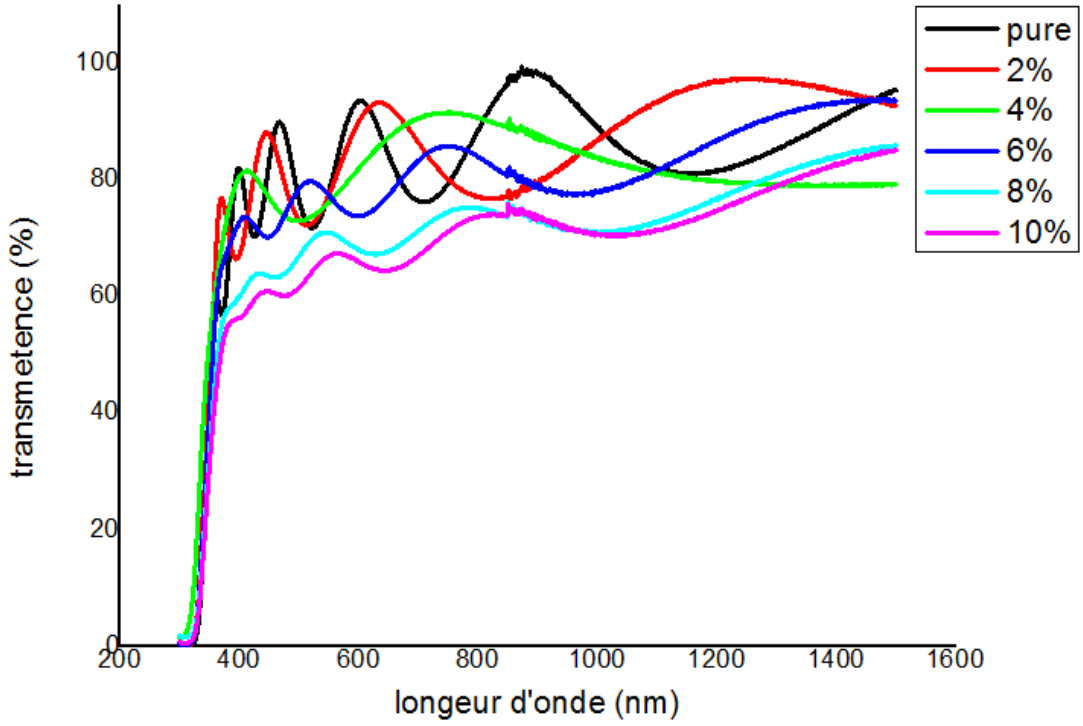


Figure III.8 : Optical transmittance spectra of $TiO_2$ thin films.

Figure (III.8) shows the variation of the transmittance of our Titanium Dioxide thin films ($TiO_2$) as a function of wavelength. There are two zones in the transmittance curve:

- Transparent zone between 350 nm and 800 nm which makes it possible to know the transmittance value in the visible domain. We note that the transmittance value of our thin films is varied between 75% and 98%. It is also observed that the transmittance decreases with the increase of the doping concentration. This decrease caused by the increase of the abserption due to the increase of opaque niobium atoms **[70]**.
- Zone of strong absorption ($\lambda$ < 350 nm) this zone corresponds to the electronic transitions between the valence band and the conduction band, this zone makes it possible to calculate the value of the band gap $Eg$ and the disorder $Eu$ **[51]**.
- According to the interference fringe as seem that the surface of our films changed from smooth to roughness films with increasing of Niobium content.

### III.2.4.2 : Optical Gap and Urbach energy:

From the values and spectra of transmittance, one can estimate the optical gap and the energy of Urbach by the method which was mentioned in the relation (II.14, II.16) in chapter 2 (with n = 2 for the direct gap) .

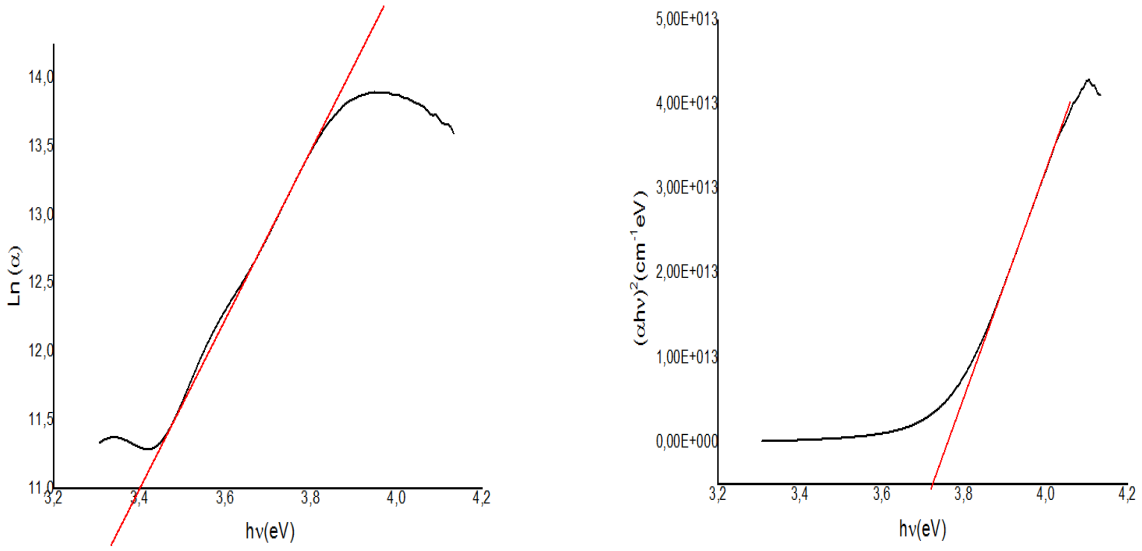


(a) (b)

Figure III.9 : Urbach energy ($Eu$) (a) and Optical gap ($Eg$) (b) for our thin filmsTiO₂.

From this method, we find the Optical gap variations and the Urbach energy as a function of niobium doping (Table III.4) .

Table III.4 : The Optical gap variations and the Urbach energy.

| concentration (Nb at%) | $Eg$ (eV) | $Eu$ (eV) |
|---|---|---|
| 0% | 3,72 | 0,15 |
| 2% | 3,71 | 0,16 |
| 4% | 3,73 | 0,19 |
| 6% | 3,70 | 0,18 |
| 8% | 3,64 | 0,18 |
| 10% | 3,65 | 0,21 |

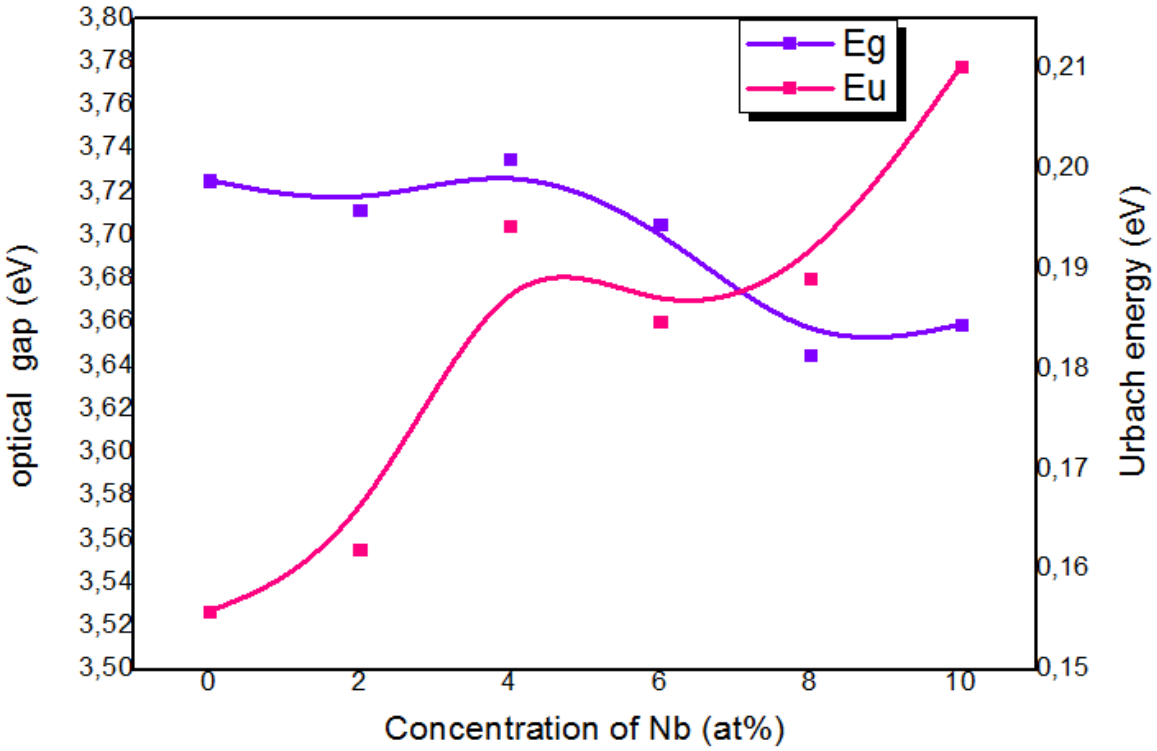


Figure III.10 : The variation of the Optical gap energy and the Urbach energy as a function of doping percentage.

The decrease in the Optical gap of our films corresponds to the improvement of the minimum energy required for the excitation of the electrons, while the electrons are easily excited towards the conduction band **[71]**. Doping by a metal is used to create an energy level in the $TiO_2$ gap. In our case, it has already been found that the energetic level of the $Nb^{+5}$ dopant is localized below the conduction band, so the electronic transition is established from the valence band to the dopant level **[72,73]**. Then, this results in a decrease in the gap with a displacement of the absorption threshold towards the visible as is already illustrated in Figure (III.8).

In addition, the Urbach energy, which reflects the width of the tails of valence or conduction bands, represents an inverse variation to that of the gap: the higher the doping rate, the more the density of localized states ( ion $Nb^{+5}$) extends deep into the gap, the more Urbach energy increases **[13]**.

## III.2.5: SEM analysis :

The surface morphology was studied by using the Scanning Electron Microscope, the SEM microstructure of the samples are given below:

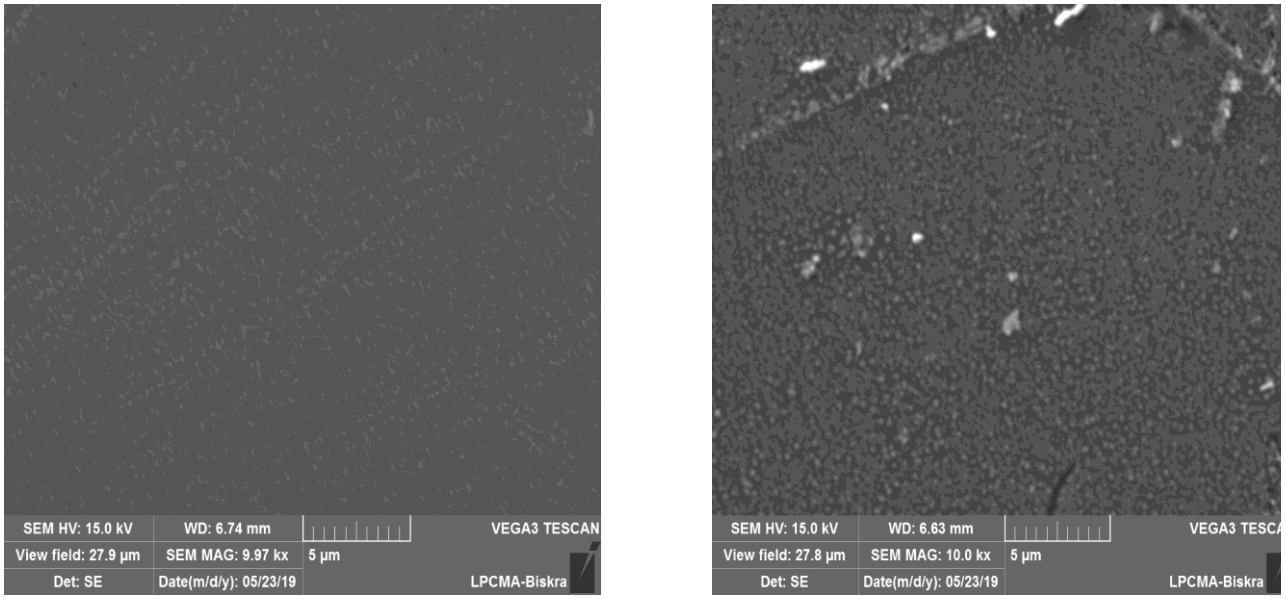


(a) (b)

Figure III.11 : SEM images of the samples (a) : Nb 0%, (b) : Nb 10%.

Figure (III.11) represent the SEM images of undoped and Nb-doped $TiO_2$. As seem that image of undoped $TiO_2$ has a smooth, dense, and compact surface however the Nb-doped $TiO_2$ has a granular surface and this results accord with C.Adomnitei et al **[74]** and A.V.Manole et al **[75]**.

## III.2.6 : The Energy X-Ray dispersive spectroscopy :

To assessment of the chemical composition of the synthesized un-doped $TiO_2$ and Nb-doped $TiO_2$ thin films the energy X-ray dispersive spectroscopy (EDS) was done and the result is shown in Fig (III.12) .

It reveals that Ti and O elements were contained in the deposited films. The high intensity of the Ti and O peaks suggest that the samples mainly contains $TiO_2$.

The main purpose of the use of technique (EDS) is the existence confirmation of Nb. All the spectra show the presence of this element, coming from the doping and we noticed an increase in the percentage of Nb with doping rate increment.

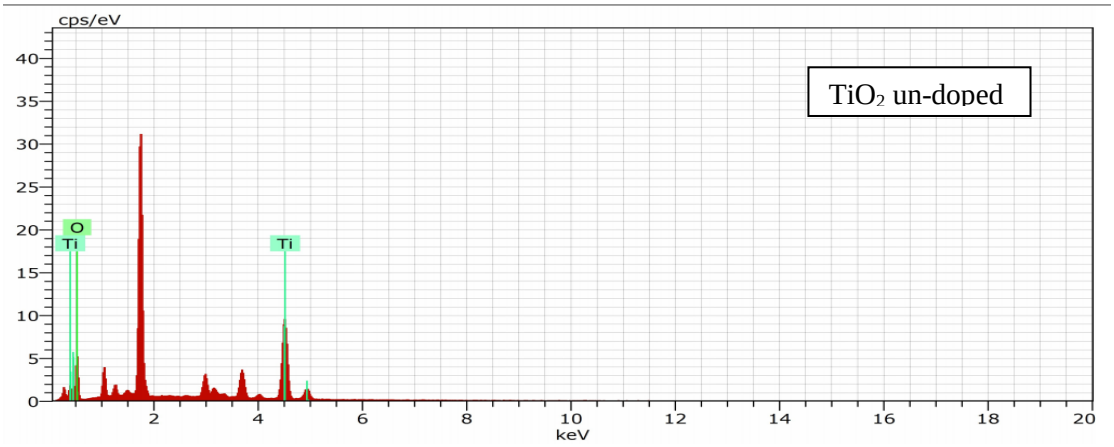


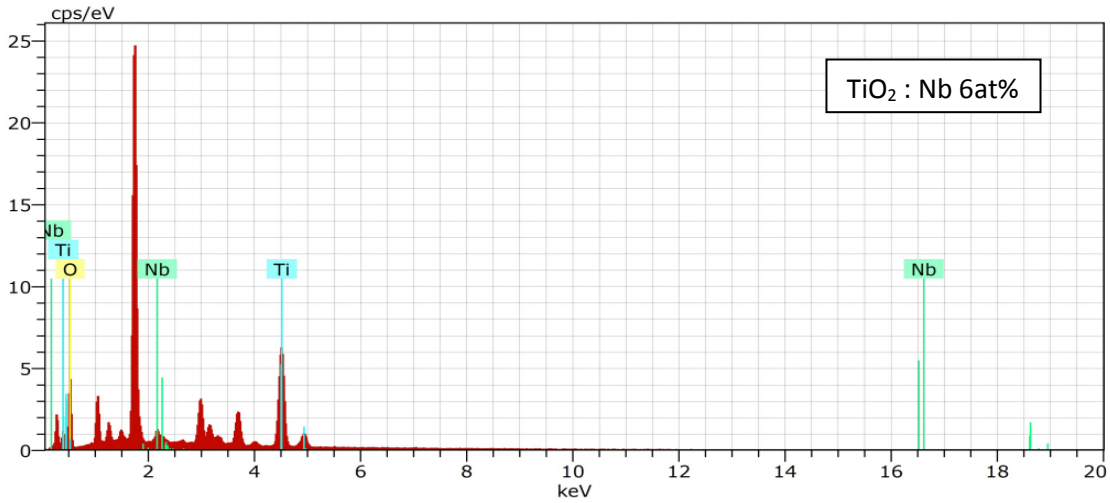


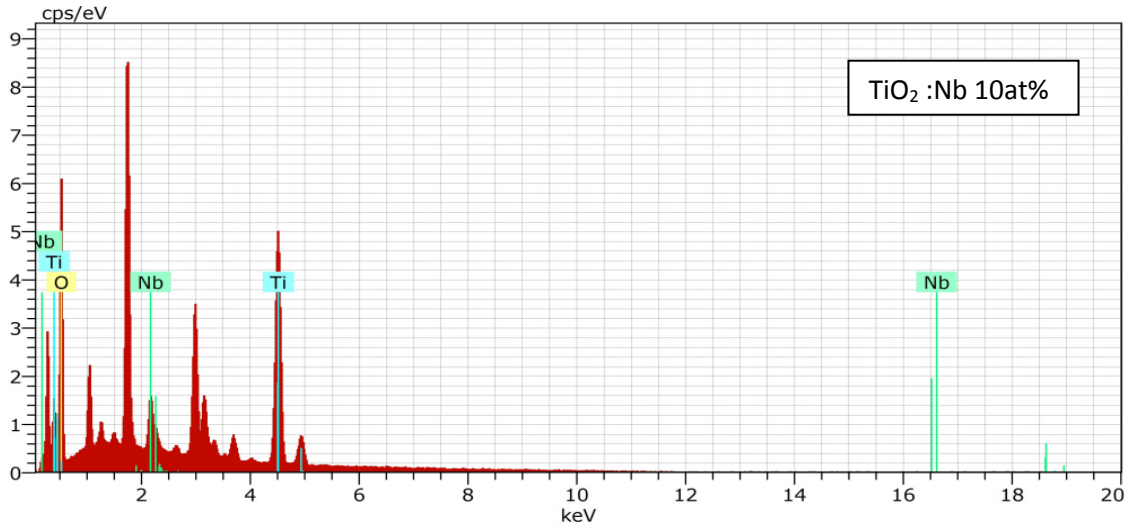


The elemental composition at the film surface obtained from EDS analysis and it is given in Table (III.5) for the samples. It can be seen the presence of the Nb atoms in the $TiO_2$ matrix.

Table III.5 : Elemental composition at the surface of samples.

| Nb % | 0% (at%) | 2% (at%) | 4% (at%) | 6% (at%) | 8% (at%) | 10% (at%) |
|---|---|---|---|---|---|---|
| O | 80.49 | 84.69 | 88.34 | 82.03 | 90.06 | 86.18 |
| Ti | 19.51 | 15.23 | 11.19 | 17.19 | 9.01 | 12.52 |
| Nb | 0 | 0.09 | 0.47 | 0.78 | 0.93 | 1.30 |
| | 100 | 100 | 100 | 100 | 100 | 100 |

## III.2.7 : Electrical properties :

For the determination of the conductivity and resistivity of our Niobium-doped $TiO_2$ films, we use the Four-point method using the relation (II.18, II.19) and the obtained results are shown in Table (III.6) :

Table III.6 : Evolution of Electrical Conductivity with doping.

| Doping rate (Nb at%) | Electrical Resistivity (ρ) (Ω-cm) | Electrical Conductivity (σ) $(\Omega\ cm)^{-1}$ |
|---|---|---|
| 0% | 0,123 | 8,118 |
| 2% | 0,062 | 16,176 |
| 4% | 0,014 | 73,426 |
| 6% | 0,071 | 14,123 |
| 8% | 0,094 | 10,649 |
| 10% | 0,042 | 24,021 |

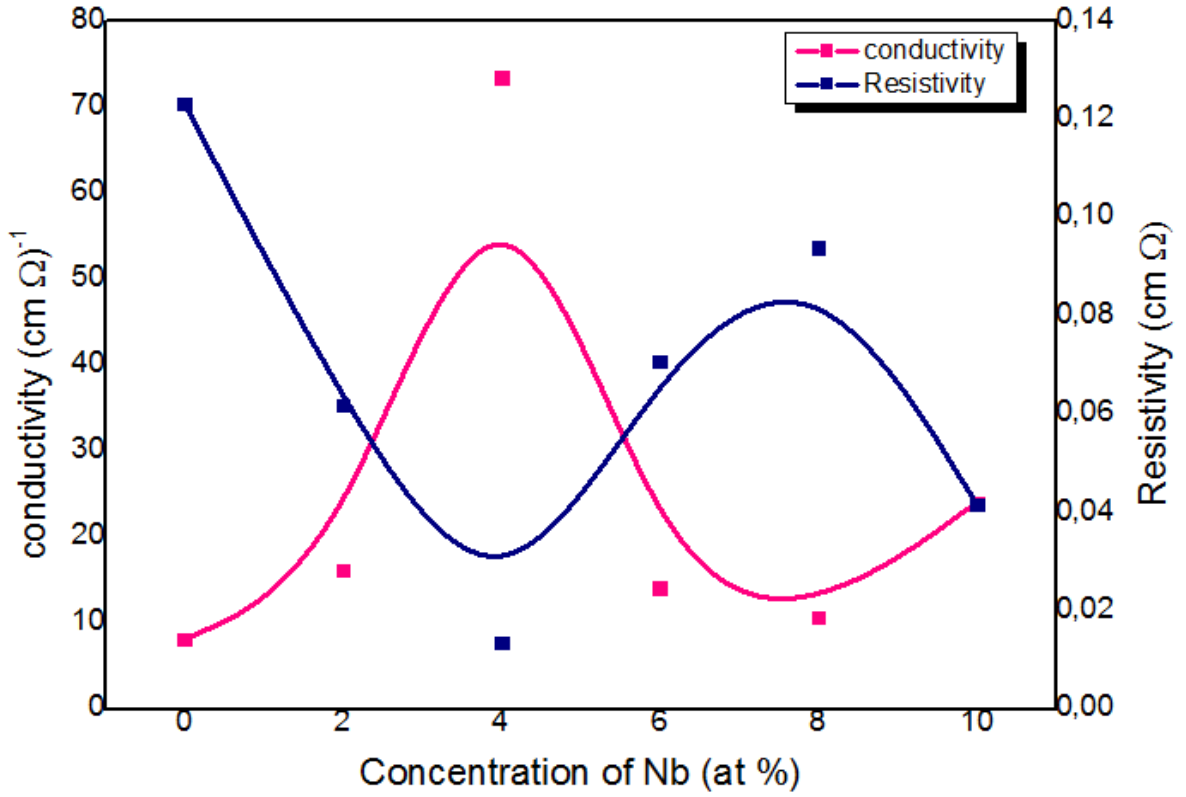


Figure III.12 : The variation of Conductivity and Resistivity as a function of the Niobium doping.

According to figure (III.12) , we can be seen a decrease of the resistivity with the increasing of Nb doping concentration until critique point 4%, after that, the resistivity of our films increase . It can explain electrical resistivity variation as follow :

In the range of 0% to 4% : the ion $Nb^{5+}$ which has an ionic radius ($R_{Nb}$ = 0.064nm**)** plus large relative to the $Ti^{4+}$ Titanium ion ($R_{Ti}$ = 0.061nm) occupies the titanium substitution sites **[56]**. In this case, the free carries number increases leaads to increase the electrical conductivity **[70]**.

In the range of 4% to 10% , the saturation of the subsutition sites and the excess of Niobium atoms play a role of scattering centers which results of the decrease of electrical conductivity.

# General conclusion

The work presented in this memory focused on the elaboration and characterization of thin films of $TiO_2$ doped with Niobium obtained by Sol-Gel (spin-coating).

We have demonstrated the influence of Niobium doping on the structural, optical and electrical properties of $TiO_2$ layers. For this purpose, a series of six samples deposited on glass substrates with different concentrations (between 0% and 10%) were prepared and Titanium Isopropoxide as precursor, Ethanol as solvent and Acetylacetone as stabilizer.

And then we characterized our samples by the following techniques: X-Ray diffraction for structural properties, UV-Visible for optical characterization and SEM for morphology and finally the Four-point technique for determining electrical conductivity.

The structural characterization by XRD shows that all the thin films of Niobium-doped $TiO_2$ obtained crystallize according to the tetragonal structure of the anatase phase with a preferential orientation towards the plane (101). The grain size varies as a function of doping from 16.72 nm to 13.92 nm and the 4% doped layer has a critical point in grain size values. The results of the optical study by UV-Visible spectroscopy show that the layers obtained have strong transmission in visible range the order of (98%). In addition, we observed a shift of absorption threshold towards the long wavelengths, due to the decrease of the optical gap from 3.69 eV to 3.65 eV with the increase of doping. The electrical characterization has shown that the niobium doping improves the electrical conductivity but is not with a large order (of the order of $10^1$ $\Omega^{-1}.cm^{-1}$) of the prepared layers.

Finally, we can say that we have succeeded in developing thin layers of undoped $TiO_2$ and doped with Niobium by the Sol-Gel technique (spin-coating) with good structural and optical properties that allow being used as optical windows.

Our perspectives are to improve the electrical properties of $TiO_2$ thin films in order to make them applicable in photovoltaic fields by using for example:

- Other doping.
- Co-doping.

# References:

**[1]** : O. Bousoum, « Etude de l'effet d'une couche mince de $TiO_2$ sur les paramètres d'une cellule solaire au Silicium », Memory of Magister, Mouloud Mammeri University, TiziOuzou, 2011.

**[2]** : I. Semahi, « Effet du traitement thermique sur les couches minces de $TiO_2$ déposé sur des support en verre », Master dissertation, Kasdi Merbah University, Ourgla , 2014.

**[3]** : V.Trinte, « Etude de théorique des phases du titane », doctorat thesis, school polytechnique, 2007.

**[4]** : M.dahnone, « Effect of annealing temperature on the properties of zinc oxide thin films deposited by Sol-Gel (spin-coating) technique », Master dissertation, Mohamed Khider University, Biskra,2015.

**[5]** : R.Ben atia , «Elaboration et caractérisation des couches minces d'oxyde de titane ($TiO_2$) obtenue par procédé Sol-Gel : l'effet de la température du recuit», Master dissertation, Mohamed Khider University, Biskra, 2016.

**[6]** : B.Said,«Elaboration et caractérisation des couches minces de Zno dopes cobalt et indium», Mohamed Khider University, Biskra, 2012.

**[7]** : F.Ynineb,«Contribution à l'élaboration de couches minces d'Oxydes Transparents Conducteurs (TCO) », Memory of Magister, Constantine University, 2010.

**[8]** : M. Long, H.J. Rack Biomaterials, 19 (1998) 1621.

**[9]** : S.zenkin, « Reactive magnetron sputtering of thin films with unique properties », doctorat thesis , West Bohemia Univarsity, Tchéque ,2017.

**[10]** : S.Christos, « Photocatalyseurs à base de $TiO_2$ préparés par infiltration chimique en phase vapeur (CVI) sur support microfibreux », doctorat thesis, National Polytechnic Institute of Toulouse, France, 2007.

**[11]** : Zahia Daas, «contribution à l'étude des propriétés de films $TiO_2$ », Master dissertation, Constantine University, 2010.

**[12]** : Subramanian, M., and al, Thin Solid Films 516.12 (2008) 3776 - 3782.

**[13]** : A. guettaf, « L'effet du dopage par l'étain sur les propriétés des couches minces de $TiO_2$ élaborées par voie Sol-Gel (sping-coating) », Master dissertation, Mohamed Khider University, Biskra, 2017.

**[14]** : O. Carp, C. L. Huisman and A. Reller , *Prog. Solid State Chem.*, 32, (2004) 33-177.

**[15]** :A.fouzia, « Etude de l'influence des effets des elements lourds sur les prorirtes physique des couches minces de $TiO_2$ », Doctorat thesis, freres mentouri University, Constantine, 2015.

**[16]** : J. F. Marucco and B. Poumellec, J. Phys. Chem. Solids, 46 (1985) 709.

**[17]** : Catherine Pighini, Doctorat thesis, Bourgogne ,2006.

**[18]** : J.guillot, « couche minces d'oxynitrure de titane : la réactivité comme moyen original de caractéresationphysico-chimique », doctorat thesis, Bourgogue Univiersity, France, 2002.

**[19]** : L. Smart, E. Moore, Introduction à la Chimie du Solide. Ed. Masson, Paris, 1997.

**[20]** :Y.Bouachiba, « Contribution à l'élaboration de l'oxyde de titane par le procédé Sol-Gel: Effet du dopage et des conditions expérimentales », Constantine University, 2014.

**[21]** : L. Börnstein, Semiconductors Physics of Non-tetrahedrally Bonded Binary Compounds, 179 (1984) 150.

**[22]** : M. Benachour, «Elaboration et caractérisation des couches minces de $TiO_2$ dopées à l'erbium, à différentes températures et épaisseurs», Master dissertation,Constantine University, 2011.

**[23]** :M.H.Samat,et al, Results in physics, 6 (2016) 891 – 896.

**[24]** : R.Mechiakh, Doctorat thesis, Constantine University, ab of céramique, , 2007.

**[25]** : B.S.Richards, « Novel uses of titanuim dioxide for silicon solar cells », Doctorat thesis, University of New South Wales Sydney 2052, Australie, 2002.

**[26]** :S.Chala, « l'effet de dopage par l'Aluminium sur les propriétés des couches minces du $TiO_2$ élaborée par voie Sol-Gel (spin-caoting) », Master dissertation, Mohamed Khider University, Biskra, 2017.

**[27]** : O .Berkani, « Elaboration et caracterisation de s couches minces d'oxyde de titane par la méthode Sol-Gel», Doctorat thesis, University Constantine1, 2013.

**[28]** : P.-C. Maness et al, Appl Environ Microbiol 65, (1999) 4094.

**[29]** : A. Mills, r. Davies, and D. Worsley, Chem Soc Rev 22, 417 (1993).

**[30]** : S. Bourgeois, P. L. Seigneur and M. Perdereau, Surface science, 328 (1995) *105*.

**[31]** : Li, Z. Zheng, et al, Nuclear instrumentation and methods in physics research B, 169 (2000) 21-25.

**[32]** : Blondeau-Patissier, Thèse de Doctorat, Dijon, 2001.

**[33]** : E. Oesterschulze, K. Masseli and R. Kassing, Fresenius' journal of analytical chemistry, 341 (1991) 70-73.

**[34]** : U. Scheithauer, W. Hösler and G. Riedl, Surface and interface analysis, 20 (1993) 519-523.

**[35]** : Lide DR (1999). Handbook of chemistry and physics .79th. edition. Chemical Rubber Company CRC press, Florida, USA.

**[36]** : M.Atoui, « Elaboration et caractérisation de couches minces de dioxyde de titane par procédé sol-gel pour des applications en photonique», Doctorat thesis, Badji mokhtar University, Annaba, 2017.

**[37]** : N.Jinesh panchal, Doctorat thesis, Sardar Patel University, 2014.

**[38]** : Cahier technologique Sol-Gel, Centre de Ressources Technologiques en Chimie, www.certech.be

**[39]** : G.Granger, « Etude et développement de fibres optiques par voie sol-gel composées de nanocristaux à base d'oxydes ($ZrO_2$, $SnO_2$). Application aux sources lasers», Doctorat thesis, Limoges university, franch, 2013.

**[40]** : A.Bazine, «Elaboration par Sol-Gel et caractérisation d'oxyde metallique (type:α-$Fe_2O_3$) aux propries photocatlytique», Memory of Magister, Constantine 1 University, 2017.

**[41]** :A.Taklit, «Dopage et caractérisation des couches minces d'oxyde de Titane( TiO2) élaborées par voie sol-gel : L'effet du taux de chlorure d'Aluminium », Master dissertation, Mohamed Khider University, Biskra,2018.

**[42]** : E.Marenna, « Sol-Gel synthesis of functional nanocomposites based on inorganic oxide», Doctorat thesis, Universityof Naples F edirico II, 2008.

**[43]** : D. Gallagher, T.A Ring, Sol-Gel processing of ceramics films Chimia, 43 (1989) 298.

**[44]** : M.Attallah, «Elaboration et caractérisation des couches minces d'oxyde de silicium, obtenues par voie Sol-Gel.», Memory of Magister, Constantine University, 2010.

**[45]** : W.Bahloul. «Génération de dioxyde de titane par réactions d'hydrolyse condensations dans une matrice polymère fondu.», Doctorat thesis, University of Claude Bernard-Lyon 1,2010.

**[46]** : S.Haya « Élaboration d'un nanomatériau mésoporeux de type nanorodsà base de dioxyde de titane ($TiO_2$), et sa mise en œuvre dans un procédé d`élimination photocatalytique des polluants organiques (PCP, MO, CV.», Memory of Magister , Annaba University , 2009.

**[47]** : M.Bahtat, « Caractérisation structurale et propriétés de couches minces de $TiO_2$ obtenues par le procédé Sol-Gel», Doctorat thesis, University Lyon 1, 1992.

**[48]** : T.Gacoin, L.Malier, J.P.Boilot, Journal of materials chemistry, 7 (1997) 859-860.

**[49]** : K.Lemounes, « Caractérisation des couches minces d'oxyde de titane ($TiO_2$) élaborées par voie Sol-Gel (spin-coating): L'effet des déférents catalyseures.», Master dissertation, Mohamed Khider University, Biskra, 2017.

**[50]** : C.A.Garcia-Gonzalez, et al, The journal of supcritical filuids, 66 (2012) 297 – 306.

**[51]** : R.Messemeche, «Caractérisation des couches minces d'oxyde de titane ($TiO_2$) obtenue par Sol-Gel (spin-coating): L'effet de la concentration de la solution.», Master dissertation, Mohamed Khider University, Biskra, 2016.

**[52]** : A.Saadi, «Rotational speed and solvent effect on the structural and optical properties of ZnO thin films prepared by Sol-Gel (Spin-coating) method.», Master Dissertation , Mohamed Khider University, Biskra, 2014.

**[53]** : A.Mockutė, « Thin Film Synthesis and Characterization of New MAX Phase Alloys», Doctorat thesis, linköping University, Sweden, 2012.

**[54]** : Dipranjan Rout,« Synthesis & Characterization of PCT (76/24) Thin Films», Master dissertation, national Institute of technology Rourkela, India, 2012.

**[55]** : A.Yahia,« L'effet de la concentration de la solution sur les propriétés des couches minces de ZnO élaborés par la méthode Sol Gel (spin-coating) », Master Dissertation, Mohamed Khider University, Biskra, 2015.

**[56]** : R.Swanepoel, journal of physic E : Scientific instruments, 1214 (1983) 16-12.

**[57]** : A.Aounali, «L'effet des substrat sur les propriétés des couche minces d'oxyde d'indium ($In_2O_3$) élaborées par spray ultrasonique», Master Dissertation, Mohamed Khider University, Biskra, 2017.

**[58]** : M.Boubeche, «Molarity Effect on the Properties of Indium Oxide Thin Films Deposited By Ultrasonic Spray Technique », Master dissertation, Mohamed Khider University, Biskra, 2011.

**[59]** : M.Amara Saâd, « Caractérisation optique et structurale des couches minces d'oxydes complexes pour applications photoniques» , Doctorat thesis , Ferhat Abbas1 University ,Sétif, 2015

**[60]** : M.Maache, « Elaboration de films minces d'oxydes semi-conducteurs par voie Sol -Gel», Doctorat thesis, Mohamed Khider University , Biskra, 2014.

**[61]** : M.Ohring, «Materials Science of Thin Films Deposition and Structure», Second Edition, Academic Press, 2002.

**[62]** : A.K.Hadi, M.H.Jaduaa, A-H.k.Elttayef, International Journal of Application or Innovation in Engineering & Management , 3 (2014) 2319- 4847.

**[63]** : M.AGolobostanfard , H.Abdizadeh, Physica B , 413(2013) 40-46.

**[64]** :M.Alzamania, A.Shokuhfara,E.Eghdama, S.Mastalib, Materials International, 23 (2013) 77- 84.

**[65]** : S .Chelbi, L. Hammiche, D. Djouadi, A. Chelouche, Rev. Alg .Phy, 2, 2(2015).

**[66]** : Y.Lu, et al, Journal of Alloys and Compounds, 663 (2016) 413- 418.

**[67]** : Panneerdoss, I.Joseph, S.Johnson Jeyakumar, and M.Jothibas, International Journal of Engineering And Science, 4 (2014) 15- 20.

**[68]** : Rahal, Achour , et al. Superlattices and Microstructures ,76 (2014) 105-114.

**[69]** : Soleimanian, S.R. Aghdaee, Applied Surface Science, 258.4 (2011) 1495- 1504.

**[70]** : H. Su et al, Electrochimica Acta 182 (2015) 230–237.

**[71]** : Huang, Fuzhi, et al, Journal of Materials Chemistry, 22.33 (2012) 17128-17132.

**[72]** : Dhanapandian, A. Arunachalam, and C. Manoharan, Applied Nanoscience 6.3 (2016) 387-397.

**[73]** : Tu, Ya-Fang, et al, Journal of Alloys and Compounds , 482.1 (2009) 382-387.

**[74]** : C.Adomnitei, D.Luca, M.Girtan, I.Sandu, V.Nica, A.V.Sandu, D.Mardare, Journal of Optoelectronics and Advanced Materials, 15 (2013) 519-522.

**[75]** : A.V.Manole ,et al, Ceramics International, 39 (2013) 4771– 4776.

# Effect of doping with thin on the properties of Titanium Dioxide thin films prepared by sol gel (spin-coating) process


## Abstract :

In this study we deposited undoped and Niobium doped Titanium Dioxide thin films with doping prcent varied btween ( 0% -10% ) onto glass substrates by Sol-Gel spin-coating method. The prepared films were obtained by dissolving Titanium (IV) Isopropoxide in a mixture of ethanol, acetylacetone, and Niobium (IV) chloride as doped source.

The films were analysed by the X-Rays diffraction (XRD), the SEM, UV-Visible spectroscopy and Four points method.

The results obtained by the XRD showed that the prepared films are polycrystalline Titanium Dioxide with a tetragonale structure of anatase. The preferential orientation is (101) and the grains size change between (16,72 nm and 13.92 nm). The UV-Visible spectrum indicated that the transmission of the films in the visible is about 90% and the gap decrease from 3.69 eV to 3.65 eV. In addition, the electrical measures showed that the films have conductivity between (8.11-73.42) $\Omega^{-1}.cm^{-1}$.



**Key words** : Thin fims, Titanium Dioxide, Sol Gel (sping-coating), Niobium, Doping.


.

# تأثير التطعيم بالنيوبيوم على خصائص الشرائح الرقيقة لأكسيد التيتان المحضرة بطريقة سائل- هلام


**ملخص :**

**في هذا العمل التطبيقي قمنا بترسيب شرائح رقيقة لأكسيد التيتان غير المطعمة والمطعمة بالنيوبيوم بنسبة تطعيم تتغير من 0 % إلى 10% على مساند من الزجاج باستعمال تقنية سائل- هلام (طريقة الترسيب باللف). الشرائح تم تحضيرها انطلاقا من محاليل رباعي ايزوبروبوكسيد التيتان المذابة في خليط من الإيثانول ، الأستيل أسيتون و خماسي كلوريد النيوبيوم كمصدر للمطعم .**

**العينات تم توصيفها باستعمال انعراج الأشعة السينية، مطيافية الأشعة فوق البنفسجية و المرئية، الميكروسكوب الماسح الإلكتروني و طريقة أربعة مسابر.**

**نتائج انعراج الأشعة السينية بينت أن الشرائح المحضرة هي لأكسيد التيتان، متعدد البلورات ذو بنية رباعية من نوع أنتاز. الإتجاه المفضل هو (101) ومقاس الحبيبات يتغير (13.92-16.72) نانومتر، منحنيات مطيافية الأشعة فوق البنفسجية والمرئية أظهرت أن متوسط النفاذية في المجال المرئي في حدود (98%)، كذلك القياسات الكهربائية بينت أن الشرائح المحضرة تتميز بناقلية متوسطة عموما بين ( 73.42-8.11 )( أوم. سم)$^{-1}$.**



**الكلمات المفتاحية : الشرائح الرقيقة ، أكسيد التيتان، سائل-هلام طريقة (الترسيب باللف) ، النيوبيوم ، التطعيم.**


# L'effet du dopage par Niobium sur les propriétés des couches minces d'oxyde de titane élaborées par voie Sol-Gel


**Résumé :**

Dans ce travail nous avons déposés des couches minces d'oxyde de titane non dopées et dopées par niobium (0% et 10 %), sur des substrats du verre par la méthode de Sol-Gel (spin-coating). Les films ont été obtenus à partir des solutions de tétra-isopropoxide de titane dissous dans un mélange de l'éthanol, l'acétylacétone et le chlorure de niobium hydraté comme source de dopant.

Les échantillons ont été analysés par la diffraction des rayons X (DRX), le MEB, la spectroscopie UV-Visible (UV-Vis) et la méthode des quater pointes.

Les résultats obtenus par la DRX montrés que les films préparés sont de l'oxyde de titane polycristallin avec une structure tétragonale de type anatase. L'orientation préférentielle est (101) et la taille des grains varie entre 16,72 nm et 13.92 nm. Les spectres de UV-Vis ont indiqué que la transmittance moyenne des films dans le visible est de l'ordre (98 %), et le gap diminue de 3.69 eV à 3.65 eV. Ainsi que les mesures électriques ont indiqué que des films préparés ont des moyennes conductivités entre (8.11-73.42) $\Omega^{-1}.cm^{-1}$.



**Mots clés** : Couches minces, Oxyde de Titane, (sping coating), Niobium, Dopage.